TALLINN UNIVERSITY OF TECHNOLOGY
SCHOOL OF ENGINEERING
Department of Electrical Power Engineering and Mechatronics

MODELLING AND SIMULATION OF ISEAUTO SELF-DRIVING VEHICLE DYNAMICS

ISEJUHTIVA SÕIDUKI ISEAUTO DÜNAAMIKA MODELLERIMINE JA SIMULATSIOON

MASTER THESIS

Student: Hennadii Onyshchenko

Student code: 184670 MAHM

Supervisor: Professor Anton Rassõlkin

Tallinn 2021

AUTHOR'S DECLARATION

Hereby I declare, that I have written this thesis independently.

No academic degree has been applied for based on this material. All works, major viewpoints and data of the other authors used in this thesis have been referenced.

"18" May 2021

Author: Hennadi Onyshchenko

　　　　/signature /

Thesis is in accordance with terms and requirements

"18" May 2021

Supervisor: Professor Anton Rassõlkin

　　　　/signature/

Accepted for defence

"......."....................20… .

Chairman of theses defence commission: ....

　　　　　　　　/name and signature/

Non-exclusive Licence for Publication and Reproduction of Graduation Thesis¹

I, Hennadii Onyshchenko (18.04.1998) hereby

1. grant Tallinn University of Technology (TalTech) a non-exclusive license for my thesis

   Modelling and Simulations of ISEAUTO self-driving vehicle dynamics,

supervised by

Professor Anton Rassõlkin,

1.1 reproduced for the purposes of preservation and electronic publication, incl. to be entered in the digital collection of TalTech library until expiry of the term of copyright;

1.2 published via the web of TalTech, incl. to be entered in the digital collection of TalTech library until expiry of the term of copyright.

1.3 I am aware that the author also retains the rights specified in clause 1 of this license.

2. I confirm that granting the non-exclusive license does not infringe third persons' intellectual property rights, the rights arising from the Personal Data Protection Act or rights arising from other legislation.

---

¹ *Non-exclusive Licence for Publication and Reproduction of Graduation Thesis is not valid during the validity period of restriction on access, except the university`s right to reproduce the thesis only for preservation purposes.*

_____ (*signature*)

_____ (*date*)

THESIS TASK

Student: Hennadii Onyshchenko, 184670 MAHM02/18

Study programme, MAHM Mechatronics

main speciality: Mechatronics

Supervisor(s): Professor Anton Rassõlkin, +37253919587

Thesis topic:

(in English) Modelling and Simulation of Iseauto Self-driving Vehicle Dynamics

(in Estonian) Isejuhtiva sõiduki Iseauto dünaamika modellerimine ja simulatsioon

Thesis main objectives:

1. Perform background research of the vehicle dynamics theory
2. Development of mathematical model in Matlab environment
3. Verify dynamics model by practical measurement and analyze received results

Thesis tasks and time schedule:

No	Task description	Deadline
1.	Finalizing of the problem statement, methods of solution, desired results and completed list of main information resources.	end of December 2020
2.	Completion of studying theory of dynamics, and also beginning of developing a mathematical model	end of February 2021
3.	Completion of mathematical model implemented in MATLAB. Testing it in practice and making conclusion in accordance to the received results	end of April 2021

Language: English   **Deadline for submission of thesis:** "18" May 2021

Student: Hennadii Onyshchenko   ……………………   "18" May 2021
                                    /signature/

Supervisor: Anton Rassõlkin   ……………………   "18" May 2021
                                    /signature/

Head of study programme: Mart Tamre   ....   "   " 2021
                                    /signature/

CONTENTS

PREFACE

Electrical self-driving vehicle is a transport of the future. Many ideas and concepts are being implemented in the ISEAUTO vehicle prototype supported by TalTech University. I am very proud to be part of this project and contributing to its development.

I would like to express my gratitude to Professor Anton Rassõlkin for assisting me with all the thesis-related questions and problems.

Also I want to thank Viktor Rjabtšikov and Ehsan Malayjerdi for help in making practical measurements.

Finally, I would like to thank my good friend and colleague Jevgeni Baklanov for moral support.

Keywords: ISEAUTO; Vehicle dynamics; Modelling and simulation; Matlab; Master Thesis

List of abbreviations and symbols

ESDC – electrical self-drive car;

EKF – extended Kalman filter;

RUKF – robust unscented Kalman filter;

KDS – kinetic dynamic suspension;

CG – center of gravity;

CV – constant velocity;

RR – rolling resistance.

1 INTRODUCTION

Electrical self-drive cars (ESDC) are vehicles used for transporting passengers and cargo without the need for drivers or fossil-fuel-driven internal combustion engines. Instead, it has artificial intelligence and electrical drive fueled by next-generation batteries.

In the modern world, we are increasingly talking about the automation of all spheres of our life since it leads to increasing efficiency and simplifying life. The same applies to developments in the field of electrical self-drive cars. The technology of ESDCs is not new, electric cars have already become a part of our daily life, but it still requires a lot of studies and improvements. According to the article [1] many leading automotive concerns such as Ford Motor, Volkswagen, Tesla give positive forecasts for this type of vehicle in the nearest future. In 2014, for the first time, electric cars received their own first official race competition, Formula E. Participating electric cars looked like a classical racing bolide and had similar technical characteristics. People's interest and popularization shows that electric cars will play a huge role in our daily life.

The coronavirus pandemic gave a new impetus to the development of this type of vehicle. Robocars, self-driving trucks, robotic carts and shuttles are used to help deliver food and medicines to isolated people. Since mid-April, Cruise, the self-driving vehicle division of General Motors Co, started to deliver food to the people in need, provided by SF-Marin Food Bank and SF New Deal. "What I do see is this pandemic really showing where self-driving vehicles can be of use in the future," [2] said Rob Grant, Cruise's vice president of government affairs.

The modern automotive industry is guided by four main factors in the design of a vehicle: safety, pollution, efficiency and price. ESDCs can help to achieve at least the first three goals. Firstly, ESDCs are totally environmentally friendly. The absence of harmful exhaust gases is a great solution for densely populated cities. Secondly, with proper preparation of the vehicle, the exclusion of the human factor from the driving process can give positive results. Thirdly, fully automated behavior of the vehicle will allow more efficient operations. As mentioned in the article [1] computer-driven cars end up with energy savings of as much as 10% simply by making better decisions about braking, accelerating and turning than human drivers.

The main advantage and disadvantage of these cars is the lack of a human factor in driving. Considering people multitasking and high workload, self-drive electric car can give opportunity drivers to do their own business while vehicle takes them to work. This means that all processes and all possible situations that arise while driving must be carefully studied and considered when designing these vehicles. An important role is

played by the dynamics of movement and behavior of the car under the influence of various internal and external factors. After all, only a deep understanding of the theory of dynamics will make it possible to correctly determine the factors that critically affect the efficiency of a vehicle.

The purpose of this work is a comparative analysis of theoretical studies of the vehicle dynamics and simulating algorithms in action, applicable to the main operations: acceleration and braking on a straight section of the trajectory.

Simulation is done in MATLAB software, where the forces will be explicit through equations of motion. The choice of the mathematical simulation algorithms of motion should be carried out using the following criteria:

     - the possibility of using a mathematical model to describe the main vehicle operations such as accelerating, braking, maneuvering;

     - actual vehicle parameters and characteristics must be considered;

     - inertial and mass characteristics of the main units of the vehicle should be considered for increasing the adequacy of the movement model;

     - the possibility of simplifying the motion model by simply excluding it from the mathematical models of individual equations and parameters.

There are many different studies and works on calculating the dynamics of a car. In this thesis, a specific case is studied on the example of the university project ISEAUTO self-drive vehicle for up to six persons.

Any model is based on assumptions, averages and simplifications. Therefore, the main task is to find the most optimal formula expressions with minimal errors. The fact is that all systems of the car are interconnected and changes in one system lead to changes in parameters for others. In this regard, some simplifications can be made. This will allow us to see and evaluate the influence of certain factors on the overall dynamics of the vehicle.

2 LITERATURE REVIEW

2.1 Basic Principles

Generally, vehicle dynamics can be described in five principles:

- Kinetic energy. This principle determines the total energy of a transport based on its mass and speed.
- Centrifugal force. This force influences the vehicle while turning and it tries to push the vehicle in the opposite direction from the conditional center of rotation.
- Inertia. This is a property of any object to resist changing the direction of movement either its in rest or in move. In my work I will use three types of inertia moments:
    a. Pitch. Force in horizontal axis. Influences on acceleration and braking.
    b. Roll. Force in lateral axis. Influences on side-to-side movement.
    c. Yaw. Force in vertical axis. The yaw angular inertia resists changing direction of the vehicle's straight movement.
- Friction. This force shows energy losses due to the resistance to motion between different surfaces. I am going to consider this force in four aspects:
    a. Static. It occurs when two touching surfaces are at rest.
    b. Sliding. It refers to the resistance of two objects sliding against each other.
    c. Rolling. It is a resistance to motion of a rolling object.
    d. Internal. It resists the movement between the particles of a material. Can be caused by either external forces or change in temperature and deformation.
- Traction. It means gripping level of tire and road surface. Can be divided into three groups:
    a. Driving traction. Occurs while accelerating.
    b. Braking traction. Occurs while decelerating.
    c. Cornering Traction. Occurs while turning.

As we can see vehicle dynamics is complicated and all forces are interconnected. Based on mentioned principles, my task is to highlight specific influencing factors that can be found directly from the vehicle specification or measured while driving. All such factors can be divided into two main groups: internal, that depends directly on the configuration of the vehicle and its constituent parts and are permanently constant all the time, as well as external ones that change depending on situations beyond our control.

Internal (vehicle characteristics) factors:

a. Drive (in our case electric motor) characteristics, such as power, torque, rotation speed and transmission losses, which determine maximum output drive power. Important thing is analyzing power and torque dependence characteristic of rotation speed value.

b. Wheel parameters, that consists of rim and tire. In this section it is important to consider the dynamic and static radius of the tire. Friction coefficient between tire and surface significantly affects the vehicle dynamic.

c. Tire and the road:
   - Location of the wheel axles relative to the center of gravity, that affects the distribution of the axle load.
   - Geometry of the car body, which determines the air resistance when driving at low and high speed.
   - Tire configuration, which includes dimensions, pressure, road grip.

External (surroundings) factors:
a. Condition of the road surface, type of surface, friction coefficient, that affects the level of adhesion and braking efficiency ratio.

b. Positive or negative surface slope, that influences the dynamics of acceleration or deceleration.

Since the behavior of a vehicle is movement of accelerating, braking, turning and driving - it is a response to forces acting on it, much of the study of vehicle dynamics should include studying how and why these forces are created. The main forces acting on the vehicle and controlling its behavior are created by the tires in contact with the road. Thus, it becomes necessary to gain a deep understanding of the behavior of tires, characterized by the forces and moments generated in the wide range of conditions in which they operate.

The dynamic behavior is determined by the forces acting on the vehicle from the tires, gravity and aerodynamics. The vehicle and its components are studied to determine what forces will be produced by each of these sources in a specific maneuver and state of balance, and how the vehicle will react to these forces.

A vehicle is made up of many components inside its outer shell. However, all these components move together. For example, when braking, the entire car decelerates as a unit; thus, it can be represented as a single concentrated mass located in the center of gravity (CG), with the corresponding mass and inertial properties. For acceleration, braking and most cornering analyzes, one mass is sufficient. For ride analysis, it is often necessary to consider the wheels as separate lumped masses. In this case, the lumped

mass representing the body is the "sprung mass" and the wheels are referred to as "unspring masses".

2.2 Existing Methods

Thesis work [3] is focused on specific internal combustion engine (ICE) vehicle.

In this work there are several approaches of how to simulate output speed over time function based on a small number of factors and dynamic forces. There are both simplified models based on Simulink environment using Simscape libraries of components for modelling and simulating mechanical systems and more sophisticated based on Matlab equations. In the simplified method many used components have predefined functions and calculations, that does not allow to fully evaluate the calculation methodology and assess the correctness of their use. The complex method includes Friction Force, Rolling Resistance Force, Aerodynamic Drag Force, Traction Force, etc. Speed to time and acceleration to time responses are compared for different types of models. This work does not consider axial loads, elasticity of springs, main tire parameters. The proposed model provides possibility of analyzing the conditions for the occurrence of oscillations under random, statistically determined external influences of road irregularities and braking parameters.

In this research work [4] an estimation of the slip angle of vehicles is made by extended Kalman filter (EKF), robust unscented Kalman filter (RUKF) and hybrid estimations. Suspension is assumed to be rigid, and its effect on vehicle dynamics, roll, and pitch is not considered. This study focuses on maneuvers on flat roads, the corresponding vertical force is negligible. The proposed RUKF is based on the vehicle dynamic model. Estimation accuracy is largely reliant on vehicle parameters, tire properties and road adhesion conditions. In severely nonlinear regions, the excessive suspension deformation and nonlinear tire slip would cause large model uncertainties, resulting that the dynamics based RUKF does not have the desired accuracy. While the kinematic-based EKF has better robustness to the modeling uncertainties. As a result, a hybrid estimation is proposed. It combines dynamic and kinematic methods for estimating the side slip angle of vehicles to make it applicable for the low and high-speed ranges. Hybrid model of vehicle slip angle is better choice for my work.

Research work [5] investigates the effect of tire pressure on the suspension state of vehicles. The situation is considered at higher and lower pressure from normal, and tests are carried out at a low speed (8 km/h). For that, a 7-degrees of freedom mathematical model was developed to analyze the time and the frequency response of the vehicle.

Research work [6] analyzes the influence of tire inflation pressure on the vehicle dynamics during braking maneuvers. Studies were done for braking on both straight and curve sections of the road. Tests were done on dry surfaces and the driver's impact was relatively small. Results show that the effect of tire inflation pressure has a significant impact on the behavior of the vehicle during braking maneuver, specifically on stopping distance for straight and curve paths, normal load of the wheels and lateral stiffness of the tire.

In this work [7] analytical models for tire traction in braking and driving is presented. It includes models with changing of the pressure distribution and without for both wet and dry surfaces. Model considers pressure distribution in the tire, contact shape, slip ratio and vehicle velocity. Main principle is to find moments of adhesion and sliding regions. Experimental tests were done for the medium speed of 30 km/h and with different loads. Comparison of theoretical model with experimental tests shows good results. This analytical model can be used in this work.

In the thesis work [8] dynamic model was divided into two sub-models: the longitudinal dynamics, which deals with the movement of the vehicle along its longitudinal axis, and the lateral dynamics, which includes the lateral displacement and the yaw rotation. For the tire model the author used popular Pacejka's Magic Formula that is fully explained in the book [9]. The main disadvantage of this formula is that it is more empiric-based rather than depends on exact tire constructions and operating conditions.

Article [10] shows how mathematical models of the car dynamic can be implemented in Matlab through coding. There are examples of models with different degrees of freedom (DOF).

Research article [11] describes kinetic dynamic suspension (KDS) system seven-DOF vehicle with conventional suspension system (VCS). The essence of this modulation is to identify the modal parameter of the vehicle. Found mass matrix can be applied to the vehicle in order to make it possible to find damping and stiffness matrices of the vehicle.

Fundamental book [12] explains all the main dynamic principles on the theoretical-practical level. It explains vehicle dynamics concepts in detail, concentrating on their practical use. Related theorems and formal proofs are provided together with real-life applications. Basic source of theoretical information that does not change with time.

[13] In this book, modeling and simulation of electric vehicles and their components have been emphasized chapter by chapter with valuable contribution of many researchers who work on both technical and regulatory sides of the field. Mathematical

models for electrical vehicles and their components were introduced and merged together to make this book a guide for industry, academia and policy makers.

In the paper [14] author suggests path planning algorithms for nonholonomic vehicles, including flatness, polynomial and symmetric polynomial trajectories considering dynamic constraints of real vehicles. The characteristics of these path planning methods are modeled and compared to evaluate more realistic and smoother trajectories. The results show that the symmetric polynomial provides the smoothest trajectory.

In the work [15] mathematical models of vehicles are developed, always considering formulating the appropriate assumptions and providing explanations for each step. This approach allows for an in-depth but simple analysis of vehicle dynamics without resorting to vague concepts. It gives clear understanding of the subject, which will be of great help both in solving problems of designing and testing new vehicles, and in solving new research topics. A new approach called MAP (Map of Achievable Performance) is presented and discussed in detail.

In the work [16] development of algorithms describing the dynamics of a car has been carried out. Considered modeling methods vehicle dynamics as an elastic-mass system, propulsion simulation and transmissions. Assumption have been developed for the rational structure and composition of the algorithm for simulating the dynamics of a passenger car in the form of interconnected subsystems of differential equations. The proposed equations of motion are the basis for creating software that allows simulating the movement of a passenger car on a computer in real time scale.

[17] In the presented work, the aim was to estimate the influence of the slipping processes of the driving axle on the main parameters of the external dynamics of the car. Time, distance and speed of acceleration of the car is examined under the condition of a changing dependence of the coefficient of adhesion on the speed of wheel slip in the contact point with the surface. To achieve this goal, a mathematical model of car acceleration was created taking into account: the variable value of the adhesion coefficient, such factors as driving moment and the moment of resistance, the distribution of normal reactions along the axes of the car with rear wheel drive. Change of the friction moment is presented in two variants of time parameter - linear and constant. Structural changes for the mass of the car are shown at different stages of acceleration. Transmission parameter is shown in conditions of changing gear ratios. The main method for solving the problem is the analytical solution of the initial differential and algebraic equations describing the movement of masses in a mathematical model (differential) and the distribution of normal reactions along the

wheels of a car (algebraic). Structural changes in the mathematical model are associated only with the variation of differential equations and their solutions.

The most complete, detailed and systematic theory of car movement is presented in the work [18]. In particular, the laws of course movement and methods for constructing models of a car as an oscillatory elastic-mass system, models of rolling a wheel with an elastic tire on uneven and flat surfaces are investigated. The loads acting on the wheel during its rolling are studied, the phenomenon of side slip of the wheel during braking is considered. The spatial elastic-mass model of a car and the equations of motion obtained on its basis are explained in detail. Consideration of a large number of design parameters in the elastic-mass model, as well as the possibility of applying the derived equations to any modes of motion allows to use these equations as a base variant of the subsystem for modeling the dynamics of a passenger car.

2.3 Conclusion

Self-drive ISEAUTO is a slow-moving vehicle with non-standard axle weight distribution. The main structural elements that should be considered:

- Two independent axles: front and rear. There are own suspension systems on each axle. On the rear axle suspension system is presented by dumper-spring and shock absorber. The front axle suspension system is presented by dumper-spring.
- Single electric drive coupled to the rear axle via a transmission.
- The transmission comprises a simple meshing of two pairs of gears together with differential. The driving force from the motor is transferred to the differential case from the input shaft via output shaft, and then distributed to the left and right drive shafts.
- Braking system consists of drum brakers on rear axle and disk brakers on front axle.

Model considered in this work is adopted in the form of a system of five bodies, which correspond to the body, connected to four wheels by elastic massless elements and dampers. The body is considered as a free rigid body and has six variations of the generalized coordinates (Figure 1.1).
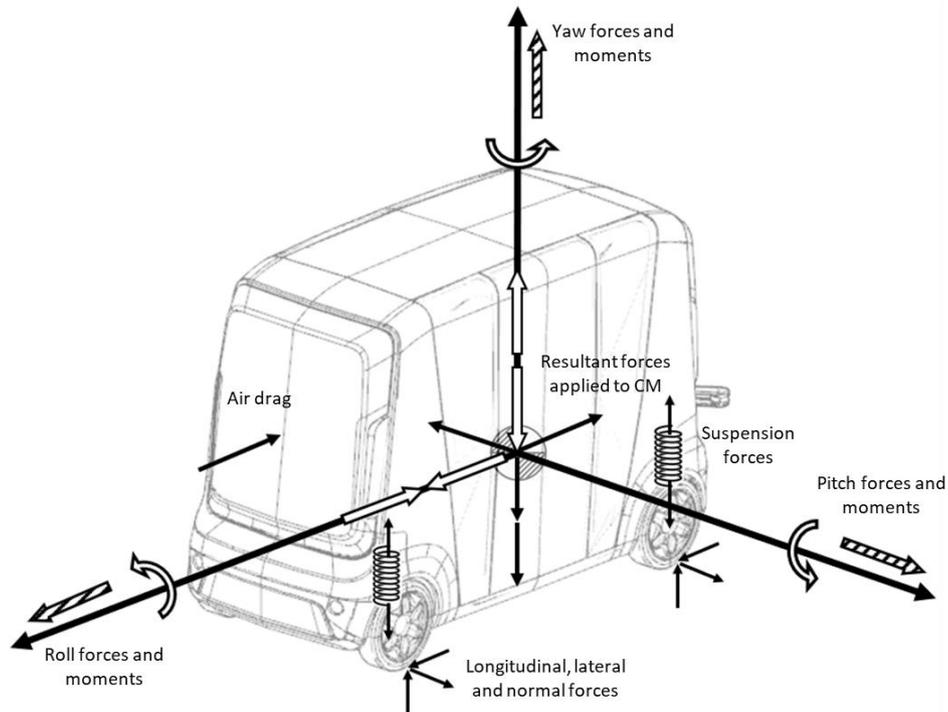
Figure 2.1 Elastic-mass model of a car

The wheels are modeled with masses concentrated at the centers of the wheels. These masses are moving only in the transverse planes. The forces of inertia acting on the wheels and corresponding to the roll of the body, and its movement in the horizontal plane are not considered. Estimated schemes for drawing up the equations of motion of unspring masses of wheels, corresponding to the assumptions are shown in Figure 2.2.
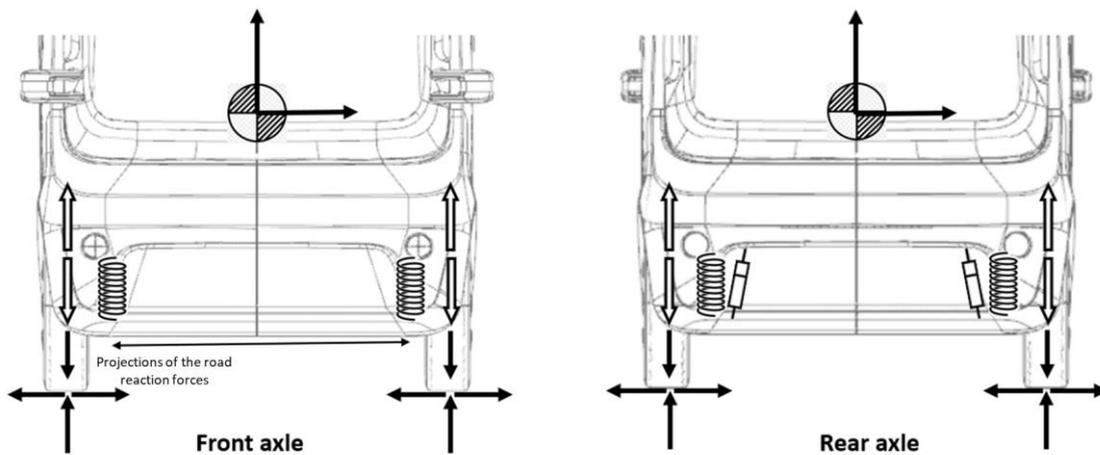

Figure 2.2 Diagrams of unspring wheel masses

The movement of the body occurs under the influence of road reactions, external active forces and forces in suspension in a frame of reference connected to the ground (Figure 1). The projections of the resultant road reactions for each wheel is done on one axis.

It is assumed that these forces are applied at the points of contact of undeformed wheels with the road surface in the static position of the vehicle and in the neutral position of steered wheels. The forces of inertia are reduced to the main vector applied in the center body gravity, and to the main moments.

Since a vehicle consists of a variety of structural units and elements with dynamically changing parameters, it is critically important to determine what should be paid attention primarily.

The acceleration of the vehicle and therefore the acceleration time depends on several main factors: the moment of inertia of the rotating motor parts and the transmission, the moment of inertia of the wheels, the transmission ratio between the transmission and the gearbox, and the torque-speed correlation. The effect of energy loss on the acceleration of the rotating mass is particularly significant for lower speeds (Figure 2.3).
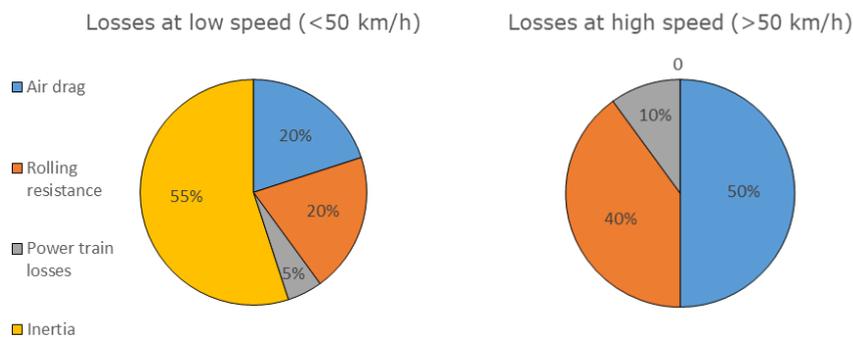

Figure 2.3 Losses proportion for low and high speed

Many studies show that at low speeds (including stop and start) the inertial forces of various components of the vehicle play a key role in losses. The rolling resistance of the tire and air resistance of the body has less but still significant influence. For the high-speed drive, the losses proportion is different. Since ISEAUTO is a low-speed vehicle, this situation is not taken into account.

All the force equations are divided into blocks for structuring and convenience. Each of them is analyzed separately. Later they will be combined into one system.
The following blocks are formed:
- Motor and transmission block. It is responsible for the characteristics of traction and energy conversion.
- Braking system block. Describes energy changes during braking.
- Acceleration system block. Describes energy changes during accelerating.

- Block for calculating longitudinal forces. It combines previous calculation blocks into one system.
- Block describing the movement of the car. It finds resulting forces of longitudinal forces.
- Vehicle movement display unit. It is used for final assessment and visualization of motion.

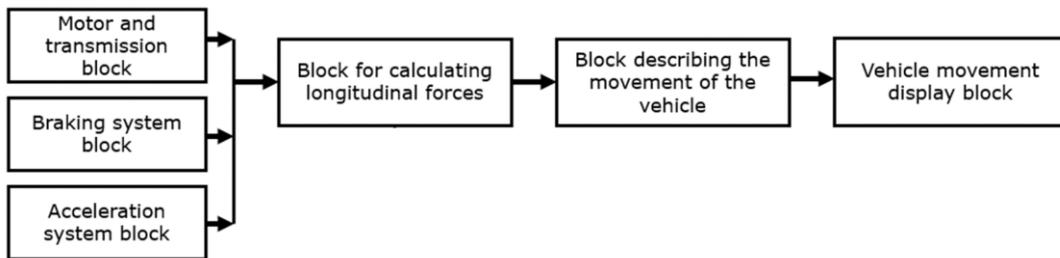The sequence and correlation of blocks is shown in Figure 2.4.

Figure 2.4 Calculation blocks diagram

Proposed model of mathematical equation blocks describes in detail elastic and inertial properties of the engine, transmission, steering and vehicle body systems. It increases the accuracy of the model to real driving conditions.

2.4 Goals and Sub-goals

Goals and sub-goals of this thesis are divided into several stages:

a. Theory stage.
- Study in detail the theory of vehicle dynamics and statics;
- define all the static and dynamic parameters that significantly influence motion;
- implement received formulas into one calculation system.

b. Modeling stage.
- Analyze different options for modeling a mathematical model;
- select the most suitable modeling option;
- implement mathematical model into Matlab;
- successfully simulate model.

c. Testing and result stage.
- Verify the correctness of the model in practice under certain conditions;
- analyze received results.

3 DEVELOPING OF THE VEHICLE DYNAMICS MODEL

3.1 Theoretical analysis

3.1.1 Motor

A motor is a device that converts certain energy into mechanical work required to make a car drive. In ISEAUTO, a permanent magnet synchronous motor (PMSM) is used for this purpose. Compared with other types of motor, PMSM performs better characteristics such as power, moment, inertia, etc.

The motor power is measured in watts or horsepower. Technical characteristics of the motor indicated either maximum rated power and speed when maximum power is reached. The time before the motor obtains maximum power directly depends on the amount of torque. The higher the torque, the faster the vehicle accelerates and the greater the traction. Torque also depends on the rotation speed of the motor shaft. For different powertrains, the peak value of the maximum torque is reached at different speeds. For some cases, this occurs in the range of 1800-3000 rpm, while for other cases-it occurs in the range of 3000-4500 rpm. The smaller these numbers are, the sooner the torque peak will arrive, which will also affect acceleration.
ISEAUTO is equipped with the Mitsubishi PMSM model Y4F1. Power characteristics are presented in the Table 3.1.

Table 3.1 Electric motor

	Model No.	Y4F1
Electric motor	Type	Permanent magnet synchronous motor
	Rated output [kW]	35
	Max. output [kW/rpm]	49/4000 – 8800
	Max. torque [N·m/rpm]	180/0 - 2500

The main characteristics of the motor are presented in the torque-speed diagram (Figure 3.1) depending on the rotational speed of the motor shaft. The ISEAUTO drive speed is selected so that the engine runs in a constant torque range.
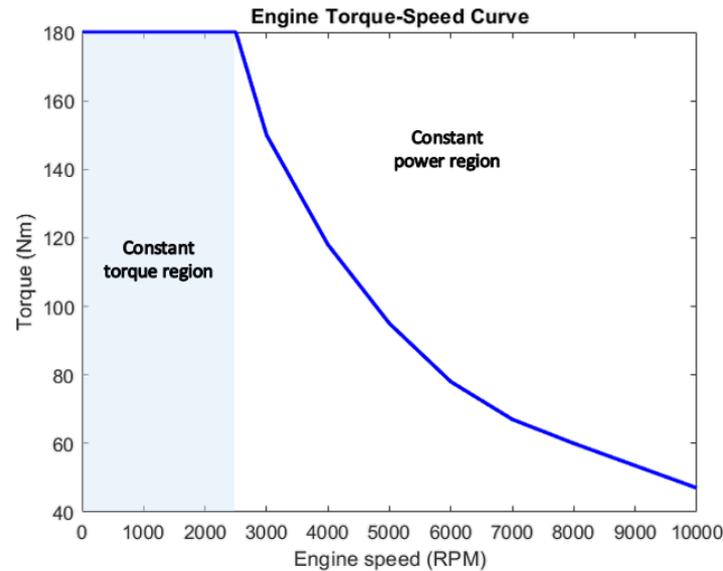
Figure 3.1 Motor torque-speed curve [22]

Since there is no possibility to measure the torque and rotation speed while driving in real time, the drive tracking occurs through the supply of a certain current and voltage. In this regard, it is also necessary to take into account the efficiency of the motor.

It is also necessary to take into account the inertia of the rotating elements of the motor. This value is measured experimentally and specified in the motor documentation. The inertia value of studied motor is chosen based on similar motors and equals to I_m = 2,884 [kg·m^2].

3.1.2 Transmission

The transmission of a car is a whole complex of mechanisms that ensures the functioning of all its driving mechanisms, transfers the energy of the motor to them. The direct purpose of the car's transmission is to step by step adjustment of torque from the power source and distribute it to the drive wheels.

ISEAUTO is equipped with mechanical transmission type (Figure 3.3). It means that power transferring between different elements is carried out by mechanical transferring of rotary motion.
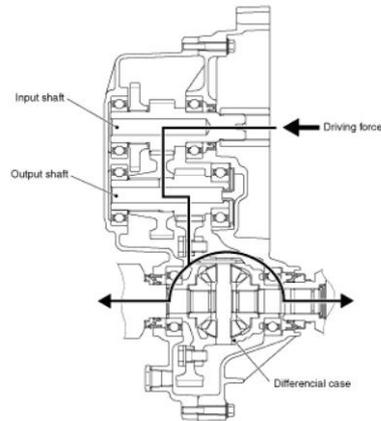
Figure 3.3 General transmission diagram

The transmission unit in ISEAUTO consists of three components:

- input and output shafts;

- gearbox;

- bevel differential.

Driving force from motor is transmitted to the input shaft of the gearbox. In the gearbox based on gear ratio, it changes parameters of torque and rotation speed. Output shaft transmits obtained new power characteristics to the differential. And differential directly distributes power to the axles with wheels. Transmission characteristics are indicated in the Table 3.2.

Table 3.2 Electric motor

Transmission model		F1E1A
Shaft configuration		Parallel shaft type two-step reduction
Overall length [mm]		172,5
Weight [kg]		19,5
Overall reduction ratio		6,066
Shift position		P - R - N - D - B - C
Transmission fluid	Brand name	Mitsubishi genuine Dia-Queen ATF SP III
	Capacity (L)	Approximately 0,75

Gearbox

A gearbox (Figure 3.4) is represented by a simple gear reduction mechanism that consist of input/output shafts and set of gears. The task of gearbox is to increase the torque transferred from the motor to the wheels. Total gear ratio (for observed gearbox it is 6.066) indicates torque increasing and rotation speed decreasing approximately in six times excluding losses.

Figure 3.4 Gearbox F1E1A

Efficiency is a key characteristic of the gearbox. The efficiency of the gearbox depends on the number of pairs of gears in mesh, parameters of the gears, type of bearings and the rigidity of the structure.

The efficiency of the gearbox can be approximately calculated theoretically using the formula:

$$\eta_{gb} = \eta_g{}^n \cdot \eta_b{}^k \cdot \eta_l, \tag{3.1}$$

where η_g - gearing efficiency of average quality gear pair (approximately 0.99),

   η_b - efficiency of bearings depends on design and quality (approximately 0.99),

   η_l - efficiency taking into account the loss of lubricating (approximately 0.98),

   n - the number of gear pairs, pcs,

   k - the number of bearings, pcs.

$$\eta_{gb} = 0{,}99^2 \cdot 0{,}99^3 \cdot 0{,}98 \approx 0{,}93$$

Gearbox efficiency slightly vary with increasing transmitted torque. In view of the fact that the motor operates in a constant torque mode, the efficiency does not change significantly. Therefore, the efficiency is taken as a constant value of 93%.

In addition to efficiency, the rotating components of the gearbox have a moment of inertia that makes them resist rotation. To calculate the total inertia of the gearbox, all assemblies are divided into separate simple elements and analyzed.
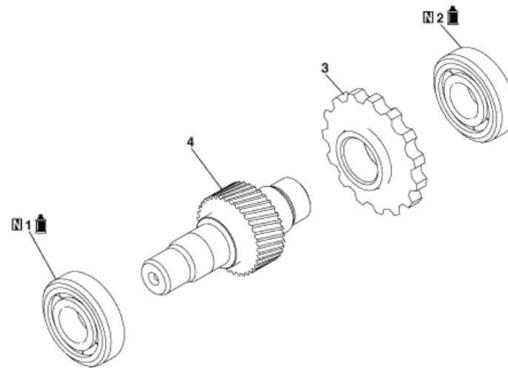
Input shaft

Figure 3.5 Input shaft [23]

Input shaft inertia is divided into three simple parts: shaft, shaft gear and parking gear (Figure 3.5). Their dimensions and weight are presented in Table 3.3.

Table 3.3 Input shaft elements

Element	Mass kg	Outer/ inner diameter mm
Shaft	1,5	30/18
Shaft gear	1	55
Parking gear	2	90

To simplify the calculation, inertia of bearings and couplings are neglected.

Shaft inertia I_{sh} is calculated by the formula of inertia of a thick-walled cylindrical pipe with inner radius r_{in}, outer radius r_{out}, and mass m_{shaft}.

$$I_{sh} = \frac{m_{shaft}(r_{in}^2 + r_{out}^2)}{2},$$

(3.2)

$$I_{sh} = \frac{1{,}5 \cdot ((15 \cdot 10^{-3})^2 + (9 \cdot 10^{-3})^2)}{2} = 0{,}23 \cdot 10^{-3}[kg \cdot m^2]$$

Shaft gear inertia I_{sg} is found as the inertia of a solid cylinder with the diameter of the gear wheel (excluding teeth) d_{sg} and mass m_{sg}.

$$I_{sg} = \frac{m_{sg}d_{sg}^2}{4},$$

(3.3)

$$I_{sg} = \frac{1 * (55 \cdot 10^{-3})^2}{4} = 0{,}76 \cdot 10^{-3} [kg \cdot m^2]$$

The same applies to parking gear inertia I_{pg} with diameter of the gear wheel d_{pg} and mass m_{pg}:

$$I_{pg} = \frac{m_{pg}d_{pg}^2}{4},$$

(3.4)

$$I_{pg} = \frac{2 \cdot (90 \cdot 10^{-3})^2}{4} = 4{,}05 \cdot 10^{-3} \ [kg \cdot m^2]$$

Total input shaft inertia I_{is} is a sum of all previously defined inertias.

$$I_{is} = I_{sh} + I_{sg} + I_{pg},$$

(3.5)

$$I_{is} = 0{,}23 \cdot 10^{-3} + 0{,}76 \cdot 10^{-3} + 4.05 \cdot 10^{-3} = 5{,}04 \cdot 10^{-3} \ [kg \cdot m^2]$$
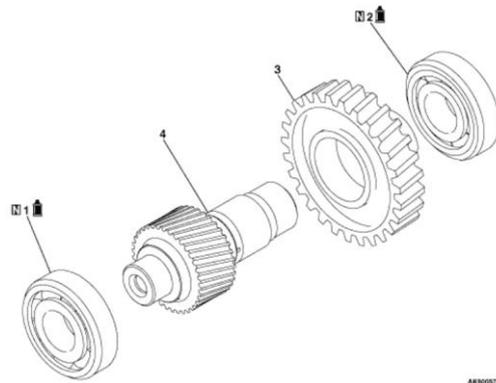
Output shaft

Figure 3.5 Output shaft [23]

Output shaft (Figure 3.5) is divided into three simple parts: shaft, shaft gear and counter gear. Their dimensions and weight are presented in Table 3.4.

Table 3.4 Output shaft elements

Element	Mass kg	Outer/ inner diameter mm
Shaft	2	40/28
Shaft gear	1,5	55
Counter gear	4	180

To simplify the calculation, inertia of bearings and couplings are neglected.
Shaft and gear inertias are calculated in the same way as for input shaft.
Output shaft inertia:

$$I_{sh} = \frac{m_{shaft}(r_{in}^2 + r_{out}^2)}{2},$$

(3.6)

where I_{sh} - shaft inertia, kg·m²,

m_{shaft} – shaft mass, kg,

r_{in} – inner radius of shaft tube, m,

r_{out} – outer radius of shaft tube, m.

$$I_{sh} = \frac{2 \cdot ((20 \cdot 10^{-3})^2 + (14 \cdot 10^{-3})^2)}{2} = 0{,}59 \cdot 10^{-3} \, [kg \cdot m^2]$$

Shaft gear inertia:

$$I_{sg} = \frac{m_{sg} d_{sg}{}^2}{4}, \tag{3.7}$$

where I_{sg} - shaft gear inertia, kg·m²,

m_{sg} – mass of shaft gear, kg,

d_{sg} – outer diameter of shaft gear, m.

$$I_{sg} = \frac{1.5 \cdot (55 \cdot 10^{-3})^2}{4} = 1.13 \cdot 10^{-3} \, [kg \cdot m^2]$$

Counter gear inertia:

$$I_{cg} = \frac{m_{cg} d_{cg}{}^2}{4}, \tag{3.8}$$

where I_{sg} - counter gear inertia, kg·m²,

m_{sg} – mass of counter gear, kg,

d_{sg} – outer diameter of counter gear, m.

$$I_{cg} = \frac{4 \cdot (180 \cdot 10^{-3})^2}{4} = 32{,}40 \cdot 10^{-3} \, [kg \cdot m^2]$$

Total output shaft inertia I_{os}:

$$I_{os} = I_{sh} + I_{sg} + I_{cg}, \tag{3.9}$$

$$I_{os} = 0{,}59 \cdot 10^{-3} + 1{,}13 \cdot 10^{-3} + 32{,}4 \cdot 10^{-3} = 34{,}12 \cdot 10^{-3} \, [kg \cdot m^2]$$

Total inertia of the gearbox mechanism I_{gb} is the sum of input and output shafts inertia.

$$I_{gb} = I_{is} + I_{os}, \tag{3.10}$$

where I_{gb} – gearbox inertia, N·m².

$$I_{gb} = 5,04 \cdot 10^{-3} + 34,12 \cdot 10^{-3} = 39,16\,[kg \cdot m^2]$$

Differential

Differential (Figure 3.6) is a mechanical device that divides the torque of the input shaft between axle output shafts. The torque from the gearbox is transmitted through a ring gear to the differential case. It rotates the axle shafts through side gears (satellites). Thus, each of the semi-axles rotates at a different angular velocity and each wheel moves freely along its trajectory without slipping.
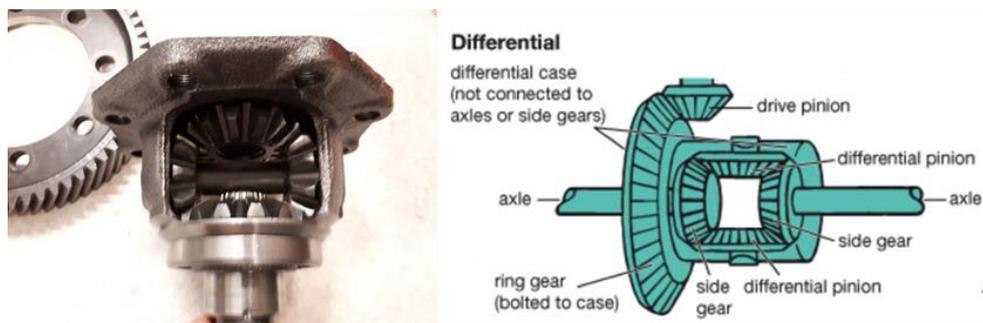

Figure 3.6 Differential design [24]

Since developed model considers only linear movement of the vehicle on a homogeneous surface, the division of the torque will be equal for both semi-axles.

Losses of the gears meshing and in the plain bearings of the semi-axial gears must be considered. The efficiency of the differential can be theoretically calculated as:

$$\eta_{dif} = \eta_{db}{}^2 \cdot \eta_{dg}{}^3, \qquad\qquad (3.11)$$

where η_{dif} – total differential efficiency,

$\quad\eta_{db}$ - efficiency of a pair of plain bearings,

$\quad\eta_{dg}$ - efficiency of a cylindrical gear pair,

In modern differential systems, the coefficients are $\eta_{db} = 0,99$ and $\eta_{dg} = 0,98$.

$$\eta_{dif} = 0,99^2 \cdot 0,98^3 = 0,92$$

For calculating the inertia of rotating elements only differential drive gear is considered. Side gears and differential pinions, due to their small sizes and masses, have

insignificant impact and are not considered in the calculations. Drive gear is presented as a solid cylinder with the diameter of the gear wheel (excluding teeth).

Table 3.5 Output shaft elements

Element	Mass kg	Outer diameter mm
Differential drive gear	3	190
2x Side gears	minor	minor
2x Pinion gears	minor	minor

Inertia of differential drive gear:

$$I_{dif} = \frac{m_{dg}d_{dg}^2}{4},$$

(3.12)

where I_{dif} - differential inertia, kg·m^2,

m_{dg} - differential drive gear mass, kg,

d_{dg} - differential drive gear outer diameter, m.

$$I_{dif} = \frac{4 \cdot (190 \cdot 10^{-3})^2}{4} = 36{,}1 \cdot 10^{-3} \ [kg \cdot m^2]$$

3.1.3 Vehicle body

Vehicle mass

Figure 3.7 ISEAUTO components under the body shell [25]

The total mass of the vehicle (Figure 3.7) is divided into two components:
- sprung mass. It consists of parts that are supported by springs or any other supporting elements of the suspension. It includes vehicle body, frame, motor, steering unit, etc.
- unsprang mass. The components of the unsprung mass include discs, tires, brakes, wheel bearings and the hubs themselves, drive shafts, axle shafts, suspension beams and axles, as well as the springs and shock absorbers.

The ratio of sprung to unsprang weight has great impact, since the force unsprung components act on the vehicle from the bottom up must be compensated by the weight of the sprung weight. Otherwise, the vehicle loses grip on the road surface, which affects its dynamics.

In addition to that, the weight of the wheels also affects the dynamics of the vehicle. The heavier the wheels, the more energy and time it will take to change its speed of rotation.

Also, the weight distribution of the front and rear-wheel drive plays an important role. If vigorous acceleration is required, then the drive wheels should be loaded as much as possible. Otherwise, the motor power will not be fully realized. During acceleration, the front wheels are unloaded, and the rear wheels are reloaded. This is especially noticeable on vehicles with a short wheelbase and high center of gravity.

In this section, the task is to determine the center of mass of the vehicle and calculate the load on each of the axes. For this ISEAUTO is divided into several components with finding the mass and coordinates of the center of mass relatively to the reference point (Table 3.6).

ISOAUTO sprung mass is divided into such subsystems:
- Vehicle shell;
- motor with transmission;
- batteries;
- steering unit;
- cargo (passengers);

In turn ISOAUTO unsprang mass consists of two elements:
- Forward axle;
- rear axle.

ISEAUTO dimensions are shown on Figure 3.8. Center point of front axle shaft is taken as reference coordinate. Coordinate values mean mm.

Table 3.6 Vehicle elements

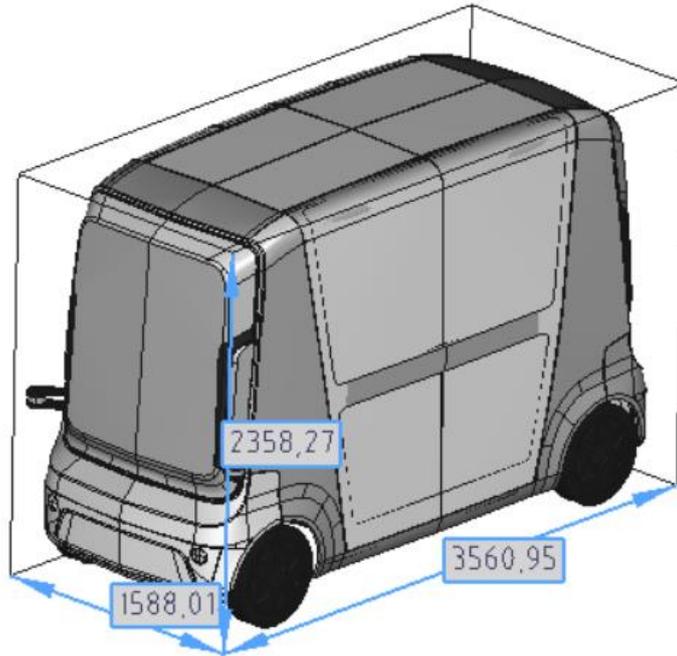| Index i	System	Mass m_i kg	Coordinates of CG $[x_i; y_i; z_i]$
1	Vehicle shell;	550	[1220;0;1540]
2	Motor, gearbox and differential	90	[2550;0;350]
3	Batteries	250	[1420;0;150]
4	Steering unit	60	[0;0;350]
5	Cargo (passengers)	0-400	[1550;0;870]
6	Forward axle	100	[0;0;0]
7	Rear axle	120	[2550;0;0]

Figure 3.8 ISEAUTO dimensions

Total mass is a sum of all defined components. For this calculation, the weight of the cargo (passengers) is chosen as 400 kg.

Total mass is:

$$m_{total} = 1570 \, [kg]$$

Unsprang mass is

$$m_{unsprang} = 1350 \, [kg]$$

Sprang mass is

$$m_{sprung} = 220 \, [kg]$$

Vehicle center of mass is calculated as:

$$[x_{cm}; y_{cm}; z_{cm}] = \frac{\sum_{i=1}^{7}(m_i \cdot [x_i; y_i; z_i])}{\sum_{i=1}^{7} m_i}, \qquad (3.13)$$

where $[x_{cm}; y_{cm}; x_{cm}]$ – coordinates of center of mass,

$\quad m_i$ – mass of each component, kg,

$\quad [x_i; y_i; x_i]$ – coordinates of each component.

After summing up all the elements from the Table 3.6, the coordinates of the center of mass for the fully equipped vehicle is:

$$[x_{cm}; y_{cm}; x_{cm}] = [1445; 0; 851]$$

29

Body dynamics

In observed model, ISEAUTO is presented as a vehicle with two axles in the conditions of longitudinal motion. Each axle has two wheels. The vehicle's center of gravity (CG) was previously defined as the center of mass.
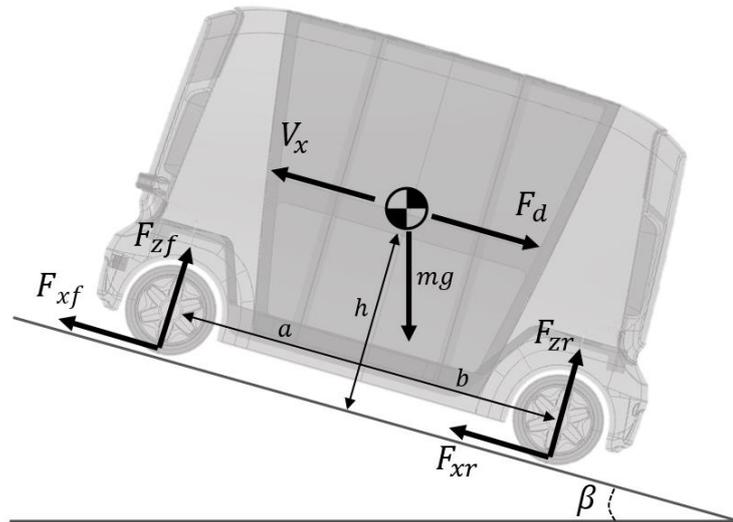

Figure 3.9 ISEAUTO dynamic model

Vehicle's weight, road inclination, aerodynamics resistance, suspension influence and axial weight distribution are considered in the presented model. It should be noted that aerodynamic resistance and weight distribution on the axle depends on the dynamic parameters of the movement. It is assumed that vehicle moves only in horizontal plane relatively to the surface.

The process of the vehicle movement is the result of the overall effect of all forces and torques applied to it. The longitudinal tire forces that occurs in the contact area of tire with surface moves vehicle forward or backward. Adhesive force is created by weight is distributed to the front and rear axles. Surface angle of inclination creates an additional projection of the gravity force pulling vehicle backward or forward. Aerodynamic traction slows down the vehicle. It is assumed that drag acts through the CG.

The equation of motion for observed model has the following form:

$$m\dot{V}_x = F_x - F_d - mg \cdot sin\beta, \tag{3.14}$$

where m – total mass of fully equipped vehicle, kg,

V_x– longitudinal velocity of the vehicle. In case positive value- forward movement, in case negative value- backward movement, m/s,

F_x – total longitudinal force on wheels, N,

F_d - force caused by aerodynamic drag, N,

β – angle of surface inclination, rad.

Total longitudinal force is the sum of forces arised on every wheel.

$$F_x = 2(F_{xf} + F_{xr}), \tag{3.15}$$

where F_{xf} - longitudinal force in contact spot with surface of front axle wheels, N,

F_{xr} – longitudinal force in contact spot with surface of rear axle wheels, N.

Vehicle mass acts on each wheel and therefore on the road. Accordingly from the side of the road there is a reaction force called normal. Since mass is not evenly distributed on the drive axes, each normal force is calculated separately.

$$F_{zf} = \frac{-h\left(F_d + mg\,sin\beta + m\dot{V}_x\right) + b \cdot mg\,cos\beta}{2(a+b)}, \tag{3.16}$$

$$F_{zr} = \frac{+h\left(F_d + mg\,sin\beta + m\dot{V}_x\right) + a \cdot mg\,cos\beta}{2(a+b)}, \tag{3.17}$$

where F_{zf} - normal load forces occurring on front axle wheels, N,

F_{zr} - normal load forces occurring on rear axle wheels, N,

a - distance from front axle to the vehicle CG, m,

b - distance from rear axle to the vehicle CG, m,

h – distance from axles to vehicle CG. It is assumed that both axles are on the same level, m.

The sum of normal forces is verified by the next equation:

$$F_{zf} + F_{zr} = mg\,\frac{cos\beta}{2}, \tag{3.18}$$

It is important to remember that at the beginning of the movement, due to the fact that the rear axle is the leading and more loaded together with the suspension impact, the

front axle tends to rise up in the form of pitch acceleration. This, in turn, affects the grip rate and, accordingly, the longitudinal forces on the wheels.

Pitch acceleration depends on three torque components and the inertia of the vehicle:

$$\alpha = \frac{(F_x \cdot h) + F_{zf}a - F_{zr}b}{I_{pitch}}, \tag{3.19}$$

where α - Pitch acceleration, m/s²,

I_{pitch} - total pitch inertia of the vehicle, kg·m².

To simplify calculation of the vehicle inertia, the inertia of each individual element from the Table 3.7 is found and then summed. The axis of rotation is the transverse axis passing through the vehicle CG. It is assumed that the mass of each element is concentrated in one point, except vehicle shell and the distance to the axis of rotation is express through the difference of their coordinates.

$$I_p = m \cdot r^2, \tag{3.20}$$

where I_p – pitch inertia of each component, kg·m²,

m - mass of element concentrated at one point, kg,

r – distance from element CG to the pitch axis of the vehicle, m.

The vehicle body has a complex geometric shape and uneven mass distribution. To determine vehicle body inertia I used the SolidWorks software by applying ISEAUTO 3D-model and mass parameters.

Inertia results are in the Table 3.7.

Table 3.7 ISEAUTO elements pitch inertia

Element	Pitch inertia kg·m²
Vehicle shell	1732,57
Motor, gearbox and differential	113,94
Batteries	316,51
Steering unit	75,96
Cargo (passengers)	25,08
Forward axle	203,01
Rear axle	151,92

Total ISEAUTO pitch inertia is a sum of all components:

$$I_{pitch} = 2799,49 \, [kg \cdot m^2]$$

In the Table 3.8 used values for calculations are presented.

Table 3.8 Used constant values for body calculations

Input	Value
m, kg	1510
a, mm	1425
b, mm	1125
h, mm	851
I_{pitch}, kg·m^2	2799

3.1.4 Drag Force

Drag force is the force that occurs when object moves through fluid surrounding (in this case- air) and it directed opposite to the movement. It caused by air resistance against the vehicle surface.

As can be found from the Figure 3.10, the effect of air resistance is not significant for driving up to 25 km/h under normal conditions. But when the moving speed exceeds 25 km/h, it is necessary to consider this force.
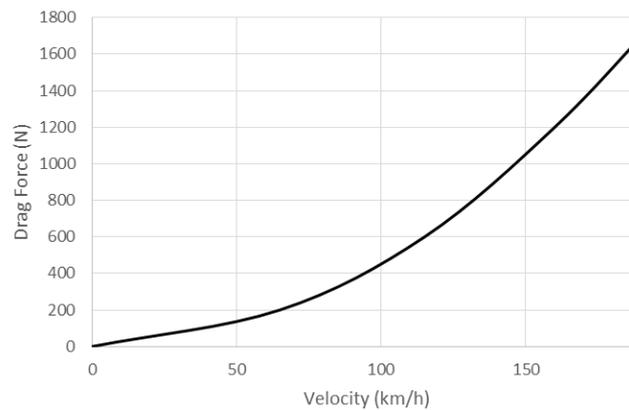

Figure 3.10 Drag Force dependency from velocity (front area 1 m^2, drag coefficient 1,0)

The drag force can be expressed as:

$$F_d = \frac{1}{2} C_d \rho A (V_x + V_w)^2 \cdot sgn(V_x + V_w),$$

(3.21)

where F_d - drag force, N,

C_d - drag coefficient,

ρ - density of air, kg/m^3,

V - flow velocity, m/s,

A - cross-sectional area of vehicle front profile, m^2,

33

V_w – speed of wind, directed to the vehicle front profile, m/s.

The aerodynamic coefficient is selected from the table of typical vehicles.

Table 3.9 Aerodynamic coefficient of typical vehicles

Type of vehicle	Aerodynamic drag coefficient
Ordinary passenger car	0.5
Bus	0,6-0,8
Truck	0,8-1,0

It is assumed that ISEAUTO frontal profile has the form of bus, consequently drag coefficient is taken as 0,7.

In the Table 3.10 used values for calculations are presented.

Table 3.10 Aerodynamic coefficient of typical vehicles

Input	Value
C_d	0.7
p, kg/m^3	1,28
V_w, m/s	0
A, m^2	3.6

3.1.5 Drive shaft

The torque from the differential to the wheels passes through the drive shafts (Figure 3.11). Inertial behavior and mechanical losses of these structural parts must be considered.

a) Rear shaft   b) Forward shaft

Figure 3.11 Rear and forward drive shafts

Drive shaft inertia moments

Inertia of drive shaft consist of shaft itself and wheel hub. For the calculation both are represented as solid cylinders.

$$I_{axle} = 2(I_{shaft} + I_{hub}) = 2\left(\frac{m_{sh} \cdot r_{sh}^2}{2} + \frac{m_{hub} \cdot r_{hub}^2}{2}\right), \quad (3.22)$$

where I_{axle} – inertia of axle, kg·m²,

   m_{sh} - mass of shaft, kg,

   r_{sh} - outer radius of shaft, m,

   m_{hub} - mass of wheel hub, kg,

   r_{hub} - radius of wheel hub, m.

Drive shaft for front and rear axles are assumed the same with the parameters shown in Table 3.11.

Table 3.11 Drive shaft elements parameters

Parameter	Value
m_{sh}, kg	4
r_{sh}, mm	10
m_{hub}, kg	7
r_{hub}, mm	140

 As a result inertia of each axle equals to:

$$I_{axle} = 2\left(\frac{4 \cdot (10 \cdot 10^{-3})^2}{2} + \frac{7 \cdot (140 \cdot 10^{-3})^2}{2}\right) = 137{,}60 \cdot 10^{-3} \, [kg \cdot m^2]$$

Driveshaft efficiency

Since the shaft is attached from one side to the differential and on the other side to the wheel hub via a constant velocity (CV) joint, mechanical losses occurs in these connections.

The overall efficiency of the driveshaft can be calculated as:

$$\eta_{ds} = \eta_{tj} \cdot \eta_{rj}, \quad (3.23)$$

where η_{tj}- efficiency of tripod joint,

   η_{rf}- efficiency of rzeppa joint.

The inner CV joint (on differential side) is a Tripod type joint, while the outer CV joint (on wheel hub side) is a Rzeppa type joint. The efficiency of these joints is around 0,99. After substituting these values into the formula, overall efficiency of the drive shaft is

$$\eta_{df} = 0,99 \cdot 0,99 = 0,98$$

In reality, the efficiency of the CV joint varies depending mostly on the offset angle between the differential and wheel. The bigger the offset, the lower the efficiency. But since the change is very insignificant, then calculated value is taken as a constant value.

3.1.6 Axle suspension

ISEAUTO is equipped with light weight and compact McPherson strut suspension system. System consists of several units, each of which has its own function:
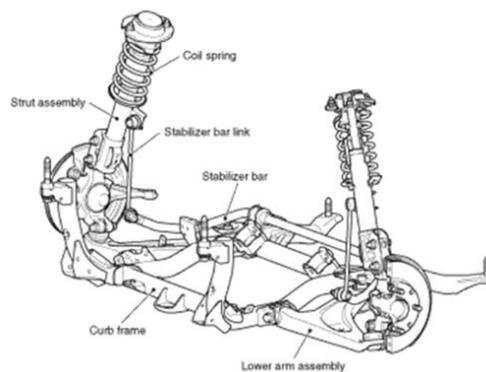
- Elastic elements. Presented as a metal coil spring.
- Shock absorbers. These are damping devices that neutralize vibrations due to unevenness, ensuring a smooth movement.
- Arms. They are responsible for the mutual movement of the wheels and the body.
- Stabilizer bars. Provides optimum rolling rigidity.

Damping effect of coil spring significantly affects the braking and acceleration dynamics of the vehicle as it plays a key role in the weight distribution to the wheels. Therefore, it is necessary to take spring stiffness into account.

Front axle suspension

a) Front suspension spring   b) Front suspension scheme

Figure 3.12 Front axle suspension

Main characteristics of front axle suspension system (Figure 3.12) are presented in the Table 3.12.

Table 3.12 Front axle suspension specification

Items		Specifications
Suspension method		McPherson strut type
Coil spring	Wire diameter, mm	10
	Average diameter, mm	77 - 96
	Free length, mm	294

Since there are two coil springs connected in series, each spring stiffness is found separately and then summed.

Stiffness of spring is calculated by the next formula:

$$k = \frac{d^4 G}{8 D^3 N},$$ (3.24)

where k – stiffness, N/m,

d - diameter of spring wire, m,

D - diameter of spring, m,

G - shear modulus of elasticity of the spring material, N/m^2,

N - number of active coils.

Used parameters stated in Table 3.13. Lower index 1 specifies upper spring, index 2 specifies lower spring.

Table 3.13 Used parameters for front axle suspension calculations

Parameter	Value
d_1, mm	10
d_2, mm	8
D_1, mm	85
D_2, mm	85
G, Pa	$82 \cdot 10^9$
N_1	7
N_2	6

Upper spring stiffeners:

$$k_1 = \frac{(10 \cdot 10^{-3})^4 \cdot 82 \cdot 10^9}{8 \cdot (85 \cdot 10^{-3})^3 \cdot 7} = 2384,3 \ [N/m]$$

Lower spring stiffeners:

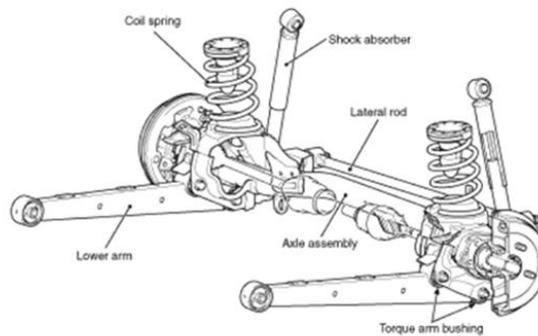$$k_2 = \frac{(8 \cdot 10^{-3})^4 \cdot 82 \cdot 10^9}{8 \cdot (85 \cdot 10^{-3})^3 \cdot 6} = 1139,4 [N/m]$$

Since two springs connected in series, total stiffness is determined from the equation:

$$k_{total} = \frac{k_1 \cdot k_2}{k_1 + k_2} = \frac{2384.3 \cdot 1139.4}{2384.3 + 1139.4} = 770,9 [N/m]$$

Rear axle suspension

a) Rear suspension photo   b) Rear suspension scheme

Figure 3.13 Rear axle suspension

Characteristics of front axle suspension system (Figure 3.13) are presented in the Table 3.14.

Table 3.14 Rear axle suspension specification

Items		Specifications
Suspension method		Torque arm type 3-link
Coil spring	Wire diameter, mm	11
	Average diameter, mm	88 to 106
	Free length, mm	307

Rear axle stiffness is calculated in the same way as front axle stiffness, but using values from Table 3.15.

Table 3.15 Used parameters for front axle suspension calculations

Parameter	Value
d, mm	11
D, mm	85
G, Pa	$82 \cdot 10^9$
N	13

The final equation is:

$$k = \frac{d^4 G}{8D^3 N} = \frac{(11 \cdot 10^{-3})^4 \cdot 82 \cdot 10^9}{8 \cdot (97 \cdot 10^{-3})^3 \cdot 13} = 1264{,}8 \ [N/m]$$

3.1.7 Tire dynamics

Tire plays a key role in vehicle dynamic, since it is the final recipient of torque and rotational speed from the motor, and element that creates a driving force.

The vehicle moves due to the force of static friction in the area of contact of the tire with the road surface. Along with static friction a rolling resistance or friction also exists. Rolling friction arises from of tire deformation. On the contrary, it slows down the movement of the vehicle. The contact patch of the tire with the road does not change relatively to the road while a tire rolling. Of course, during rolling in the contact patch there are always tire tread elements that slip relatively to the road, but in the case of uniform linear movement of the vehicle, they can be ignored and the friction force can be considered as the static friction force. When braking, most of the tire tread elements slide along the road surface. In this case, the rotation of the wheel (and therefore the vehicle) is braked by the sliding friction force. It should be noted that usually the sliding friction force is less than the static friction force.

Developed tire dynamic model is presented by tire with longitudinal linear motion. Main longitudinal movement calculations are done using the Magic Formula method. This method does not have precise physical basis. Instead it uses empirical parameters responsible for the objective characteristics of the tire, road surface and their interaction. Each element is described by several coefficients for each force it produces at the contact patch. The advantage of this method is to simplify very complex calculations without significant errors.

To increase the accuracy of the tire model, some properties are specified such as tire compliance, inertia, and rolling resistance.

The tire longitudinal direction is the same as direction of motion as it rolls on surface. Tire normal force is applied perpendicularly to the surface.
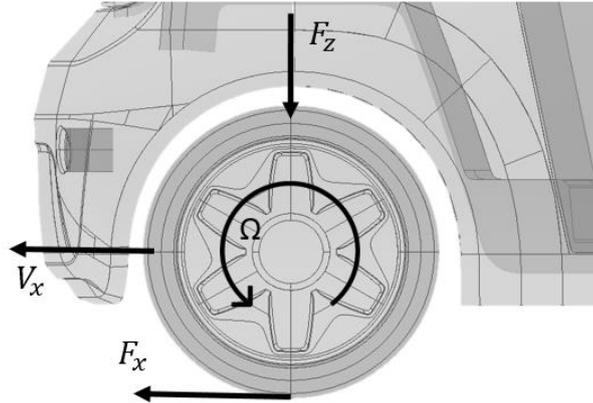
Figure 3.14 Tire dynamic model

An ideal tire without slipping moves according to the next formula:

$$V_x = r_w \cdot \Omega, \qquad (3.25)$$

Where V_x – longitudinal velocity, m/s,

r_w – wheel radius, m,

Ω – wheel angular velocity, rad/s.

Since tires always have slip, they creates a longitudinal force. Considering this, the wheel slip velocity can be calculated as:

$$V_{sx} = r_w \cdot \Omega - V_x, \qquad (3.26)$$

Where V_{sx} – longitudinal slip velocity, m/s.

The wheel slip is a ratio of longitudinal slip velocity and ideal longitudinal velocity.

$$k = \frac{V_{sx}}{|V_x|}, \qquad (3.27)$$

The general representation of the Magic Formula developed by Pacejka, is:

$$F_x = F_z \cdot D \cdot sin\big(C \cdot arctan(Bk - E(Bk - \arctan(Bk)))\big), \qquad (3.28)$$

where F_x – longitudinal force, N,

B, C, D, E - Magic Formula coefficients.

Magic Formula coefficients are based on empirical tire data. These values are presented in sets for typical road surfaces (Table 3.16).

Table 3.16 Magic Formula coefficients for typical surfaces

Surface	B	C	D	E
Dry tarmac	10	1,9	1	0,97
Wet tarmac	12	2,3	0,82	1
Snow	5	2	0,3	1
Ice	4	2	0,1	1

The rolling resistance (RR) of a tire depends on three factors:
- Energy loss of tire material as a result of cyclic deformation of the rolling tire;
- frictional energy in the contact patch;
- air resistance.

More than 90% of the RR is generated by the first factor, and energy loss in a tire is thus most important in terms of dynamic analysis.

Rolling resistance coefficient is the ratio of the rolling resistance force to the resultant longitudinal force at the contact patch:

$$f_r = \frac{F_r}{F_x},$$ (3.29)

where f_r – resistance coefficient,

F_r - rolling resistance force at the contact patch, N,

F_x - longitudinal force at the contact patch, N.

Rolling resistance coefficient can be calculated using the following empirical formula dependency from tire longitudinal velocity:

$$f_r(V) = \tilde{F}_{r1} + \tilde{F}_{r2}\frac{V_x}{100} + \tilde{F}_{r3}\left(\frac{V_x}{100}\right)^4,$$ (3.30)

where $f_r(V)$ - rolling resistance coefficient,

$\tilde{F}_{r1}, \tilde{F}_{r2}, \tilde{F}_{r3}$ - empiric coefficients.

f_r value usually is in the range of 0,005–0,015. Coefficients $\tilde{F}_{r0}$, $\tilde{F}_{r1}$ and $\tilde{F}_{r3}$ depend on the type of tire and the pressure in the tires. ISEAUTO tires have the next coefficients:

$\tilde{F}_{r1} = 9{,}0 \cdot 10^{-3}$,

$\tilde{F}_{r2} = 2{,}0 \cdot 10^{-3}$,

$\tilde{F}_{r3} = 3{,}0 \cdot 10^{-4}$.

Dependency analysis of rolling resistance from speed shows that for 0-20 km/h coefficient is constant 0,009 and only by 50 km/h it rises to 0,0092. Since IEAUTO is a slow moving vehicle rolling resistance coefficient is assumed to be constant with value 0,009.
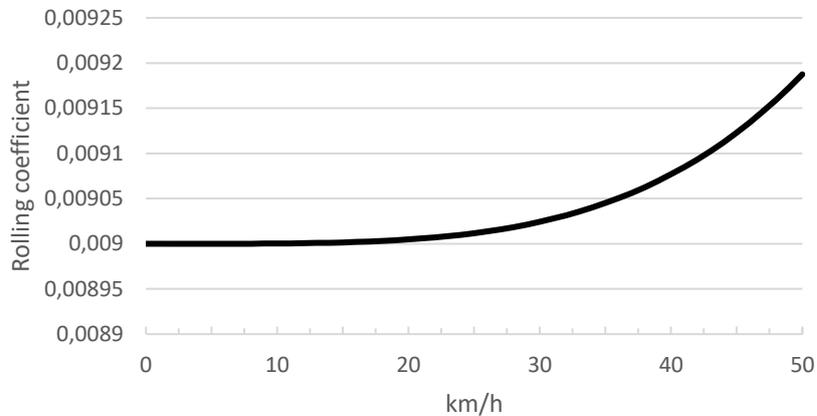

Figure 3.15 Rolling resistance coefficient dependency from velocity

The next important parameters of the tire is its size. There are several types of size parameters that are used in the calculations:

- Car wheel radius. Specified in tire description;
- free radius. Radius of wheel in the absence of external forces;
- static radius. Distance from the centre of a stationary wheel to the contact patch, loaded only with normal force;
- dynamic radius. Distance from the centre of the rolling wheel to the contact patch. Depends on the forces and moments acting on the wheel.

According to the manufactures data, front tires marked as 145/65R15 72S and rear tires marked as 175/55R15 77V.

Static radius is found by next formula:

$$r_s = \frac{d}{2} + H * \lambda, \qquad (3.31)$$

where r_s – static radius of the tire, m,

d - diameter of the tire disk, m,

H - tire profile height, m,

λ - loading coefficient (for diagonal tires 0,85-0,9; for radial tires 0,8-0,85).

After substitution of values result is:

$$r_s = \frac{0.38}{2} + 0,96 \cdot 0,85 = 0,27 \ [m]$$

Front tire inertia:

$$I_{ftire} = \frac{m_{ftire}(\text{r}_{\text{f}0}^2 + \left(\frac{d_f}{2}\right)^2)}{2}, \tag{3.32}$$

Where I_{ftire} – front tire inertia, kg·m^2,

$\qquad m_{ftire}$ – front tire mass, kg,

$\qquad r_{f0}$ – front tire wheel radius, m,

$\qquad d_f$ – front tire disk diameter, m.

$$I_{ftire} = \frac{7 * ((285 \cdot 10^{-3})^2 + (381 \cdot 10^{-3})^2)}{2} = 406,6 \cdot 10^{-3} \ [kg \cdot m^2]$$

Rear tire inertia:

$$I_{rtire} = \frac{m_{rtire}(\text{r}_{r0}^2 + \left(\frac{d_r}{2}\right)^2)}{2}, \tag{3.33}$$

where I_{rtire} – rear tire inertia, kg·m^2,

$\qquad m_{rtire}$ – rear tire mass, kg,

$\qquad r_{r0}$ – rear tire wheel radius, m,

$\qquad d_r$ – rear tire disk diameter, m.

$$I_{rtire} = \frac{10 * ((285 \cdot 10^{-3})^2 + (381 \cdot 10^{-3})^2)}{2} = 288,6 \cdot 10^{-3} \ [kg \cdot m^2]$$

3.1.8 Braking system

When breaking signal is sent, hydraulic electrical vacuum pump creates pressure in the brake pipes (Figure 3.15). Fluid pressure acts on the pistons of the working brake cylinders on brake disc that presses the pads against it. It reduces speed due to frictional force and consequently leads to braking of the vehicle. The design of the brakes, the characteristics of their elements and the pressure generated by the hydraulic pump affect the smoothness and speed of braking.
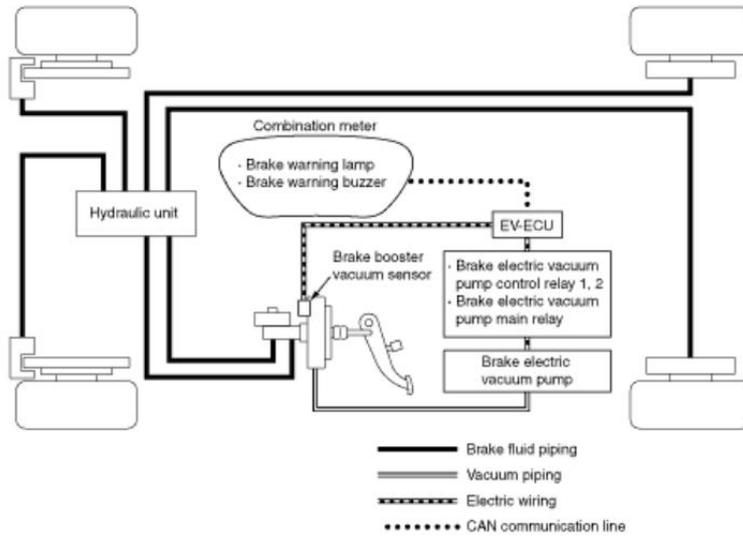
Figure 3.15 Electrical vacuum braking pump diagram

When modeling vehicle braking, it is important to consider a geometric parameters of the braking pad, pressure applied to it together with static and kinetic friction coefficients between the disc and the pad.

Front breaking system

Front breaking system is equipped with floating caliper one piston ventilated disc (Figure 3.16). Brake disc characteristics are presented in Table 3.17.
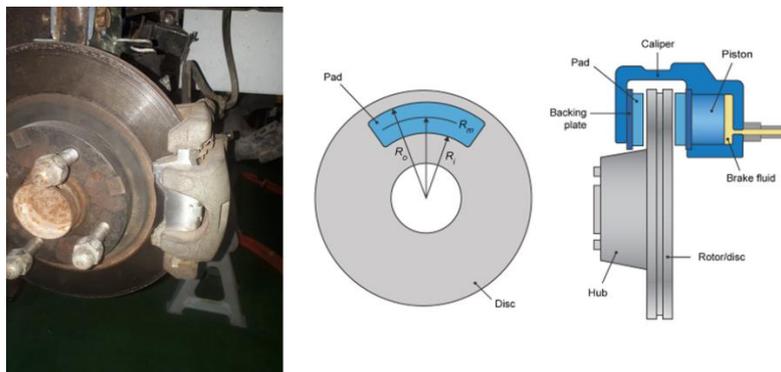

Figure 3.16 Front breaking system design

Table 3.17 Front breaking system specification

	Type	Floating caliper 1 piston ventilated disc
Front brake	Disc dimension (Outer diameter × thickness) mm	257 × 17
	Cylinder diameter mm (Number of pistons)	51,1(1)
	Brake pad thickness mm	10,0
	Gap adjustment	Automatic adjustment

Breaking fluid transfer pressure to the piston that pushes breaking pad at mean radius to disk. Maximum possible pressure according to the breaking pump specification is 10.8 MPa. Accordingly, depending on the breaking signal value, the applied pressure is the range of 0-10.8 MPa.

Friction moment depends on wheel speed of rotation. If rotation speed Ω is greater than 0, then for finding breaking moment kinetic friction is used:

$$T = \frac{\mu_k P \pi D_b^2 R_m N}{4},$$ (3.34)

where T - brake torque, N*m,

μ_k - kinetic friction between disc and pad,

P - brake pressure, Pa,

D_b - actuator bore diameter, m,

R_m - mean radius of brake pad, m,

N - the number of brake pads.

If rotation speed Ω equals to 0 meaning that vehicle does not move, then for finding breaking moment static friction is used:

$$T = \frac{\mu_s P \pi D_b^2 R_m N}{4},$$ (3.35)

where μ_s - static friction between disc and pad

Mean radius of brake pad is:

$$R_m = \frac{R_0 + R_i}{2},$$ (3.36)

where: R_0 - outer radius of brake pad, m,

R_i - inner radius of brake pad, m.

Static friction occurs between surfaces that does not move relatively to each other. Kinetic friction or dynamic friction in contrast occurs when two objects move relative to

each other. Usually the static friction is bigger than kinetic friction coefficient for the same materials. The breaking pads installed on the ISEAUTO are type E, meaning that static friction coefficient is in the range of 0,25-0,35 (Table 3.18).

Table 3.18 Friction coefficient of pad types

Type	Friction coefficient
C	Less 0,15
D	0,15 – 0,25
E	0,25 – 0,35
F	0,35 -0,45
G	0,45 – 0,55
H	0,55 – 0,8

All the parameters used in front breaking calculations 3,32 – 3,34 are presented in the Table 3.19.

Table 3.19 Front breaking calculations parameters

Parameter	Value
P, MPa	0-10,8
N, pcs	1
μ_s	0,30
μ_k	0,25
D_b, mm	51,1
R_m, mm	17
R_0, mm	257
R_i, mm	240

Rear breaking system

ISEAUTO is equipped with drum braking system on rear axle. Its parameters are shown in Table 3.20.

Table 3.20 Front breaking calculations parameters

	Type	Leading-trailing
	Drum inner diameter, mm	203.0
Rear brake	Wheel cylinder diameter, mm (inch)	19,1(3/4)
	Thickness of lining, mm	4,0
	Gap adjustment	Automatic adjustment

A drum brake is a type of brake system that consists of a rotating drum in which braking is achieved by pressing the brake pads against the drum (Figure 3.17). The main elements of a drum brake mechanism with a hydraulic drive are:
- brake pads that directly brake and linings of friction made of material with high friction coefficient;
- brake drum;

- brake cylinders, under fluid pressure in the hydraulic system presses the pads against the inner surface of the brake drum. All these parts are mounted on a base shield.

The drum break equipped on ISEAUTO represents double-shoe brake with two (leading and trailing) shoes located on both sides of the retraction spring. Such design allows significantly increase the contact area, which directly affects the braking speed. Expander force from the hydraulic pistons presses boss shoes to the rotating drum. The resulting contact frictional force between shoes and drum surfaces causes decelerating of the rotating drum.
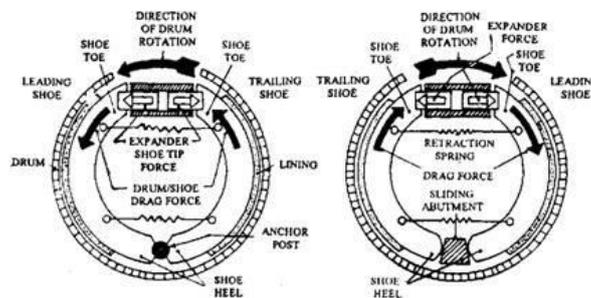

Figure 3.17 Drum breaking system design [26]

Braking torque on the leading and trailing shoes may differ because of geometry properties and applied pressure distinctions. Accordingly, torque on each shoe is calculated separately. Braking torque on the leading shoe is calculated by formula:

$$T_{ls} = \frac{c\mu p_a r_D^2 (cos\theta_{sb} - cos\theta_s)}{sin\theta_a},$$
(3.37)

where T_{ls} - braking torque arised on the leading shoe, N*m,

c - cylinder force arm, m,

μ - contact friction coefficient,

p_a - pressure applied to the leading shoe, Pa,

r_D - drum radius, m,

θ_{sb} – angle between shoe attachment pin and shoe contact point, deg,

θ_s – angle of the shoe, deg,

θ_a - angle between shoe attachment pin and pressure point, deg.

Braking torque on the trailing shoe is calculated as:

$$T_{ts} = \frac{c\mu p_b r_D^2 (cos\theta_{sb} - cos\theta_s)}{sin\theta_a}, \qquad (3.38)$$

where T_{ls} - braking torque arised on the trailing shoe, N·m,

p_b - pressure applied to the trailing shoe, Pa.

Cylinder force arm is calculated using the formula:

$$c = r_a + r_p cos\theta_p, \qquad (3.39)$$

Where: r_a - distance from the drum centre and actuator, m,

r_p - distance from the drum centre and shoe attachment pin, m,

θ_p - angle between shoe attachment pin and vertical axis of the drum, deg.

The total frictional torque of the drum breaking system is:

$$T = T_{ls} + T_{ts} + \mu_{visc} \cdot \omega_{shaft}, \qquad (3.40)$$

where T – total braking torque, N·m,

μ_{visc} - viscous friction coefficient.

All the used parameters for rear braking system calculations 3,35 – 3,38 are shown in Table 3.21.

Table 3.21 Front breaking calculations parameters

Input	Value
μ	0.30
μ_{visc}, N·m/(rad/s)	0.01
$p_a = p_b$, MPa	0-10,8
r_D, mm	101
θ_{sb} , deg	5
θ_s , deg	120
θ_a , deg	90
r_p ,mm	90
θ_p , deg	15
r_a , mm	75

3.2 Matlab and Simulink arrangement
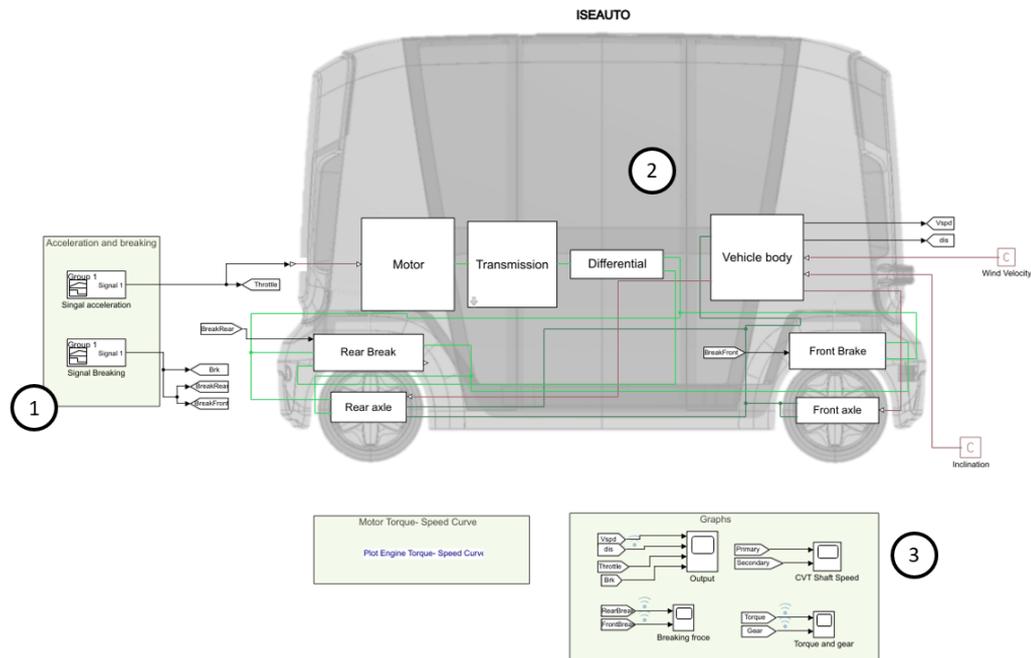
3.2.1   General model

Figure 3.18 Simulink general model

The graphical representation of dynamic mathematical model of ISEAUTO implemented in Simulink environment is shown on Figure 3.18. Presented vehicle model allows setting the parameters and conditions separately for each individual element.

In section 1 there are signal sources responsible for the conditional pressing of the gas and brake pedals. Their values are in the range of 0 and 1, which corresponds to no pressing and applying full force to it. The change in the value of the signals occurs over time and the necessary data are easily obtained experimentally.

In section 2 contains the main control units. For ease of use, they were divided into systems: motor, transmission, differential, vehicle body, front and rear axles, front and rear braking systems. Each of the subsystems is described more detailed in the sections below.

In section 3, the main graphs of the vehicle's movement are displayed.
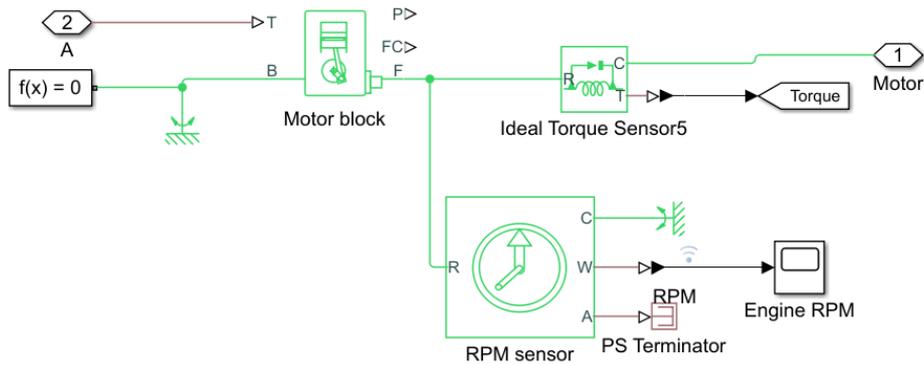
3.2.2   Motor

Figure 3.19 Simulink motor model

This subsystem (Figure 3.19) is responsible for vehicle propulsion and presented by electrical motor. The motor generates a certain torque and rotation speed depending on the integrated torque-speed curve presented in section 3.1.1. The model takes into account the rotor inertia. The rest of the blocks are responsible for transforming and reading data.
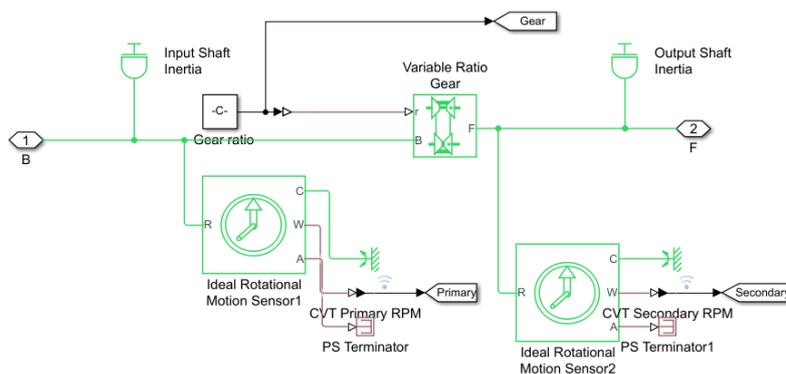
3.2.3   Transmission

Figure 3.20 Simulink transmission model

The transmission (Figure 3.20) is represented by a gearbox, which in this case has a constant gear ratio, inertia and efficiency. It should be noted that, if necessary, the gear ratio can vary depending on the conditions. The rest of the blocks are responsible for transforming and reading data.
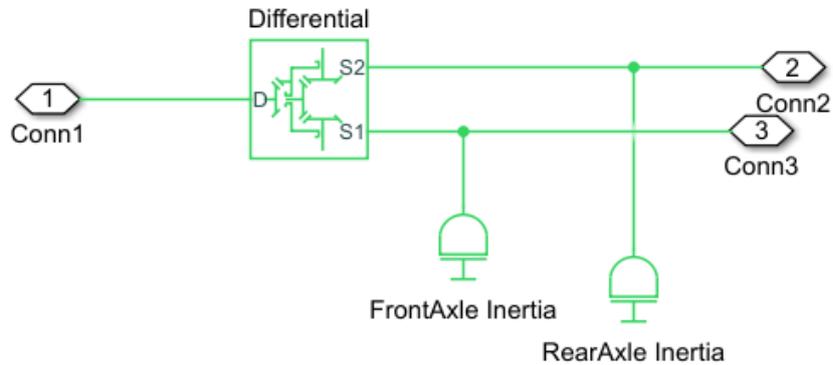
3.2.4   Differential

Figure 3.21 Simulink differential model

Block subsystem (Figure 3.21) is responsible for differential with the characteristics of carrier to driveshaft teeth ratio, as well as inertia. This block also includes the inertia characteristics of the rear and front axles.

3.2.5   Vehicle body

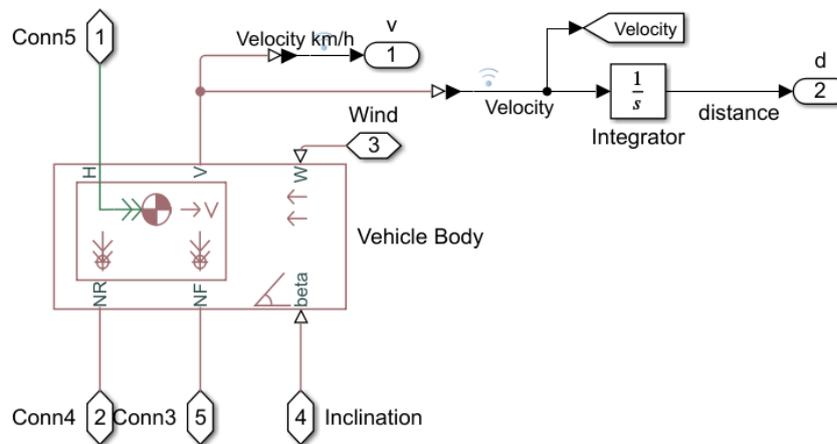Figure 3.22 Simulink vehicle body model

This subsystem (Figure 3.22) consists of a machine body presented as a solid body with specified mass-geometric characteristics, namely, dimensions, location of the center of mass, mass load on each of the axes and aerodynamic parameters. The specified block receives information about the torque from each axis, the inclination of the surface and environmental parameters.

3.2.6   Rear braking system

Figure 3.23 Simulink rear breaking system model

The rear axle wheel braking subsystem (Figure 3.23) is represented by drum brake units with two braking elements. The moment of resistance caused by them depends on the maximum possible value of the pressing force, limited by the technical parameters of the brake system based on the Mitsubishi, as well as the proportion of pressing the pedal. Geometric parameters, static and kinetic friction coefficients used in the model are indicated in section 3.1.8. The rest of the blocks are responsible for transforming and reading data. The braking units are coupled to and resist the torque vector from the engine.

3.2.7   Front Braking system

Figure 3.24 Simulink front breaking system model

The subsystem of braking the wheels of the front axle (Figure 3.24) is presented by analogy with the braking system of the wheels of the rear axle. The only difference is the replacement of drum brakes with disc brakes with a corresponding change in the geometric and friction parameters.
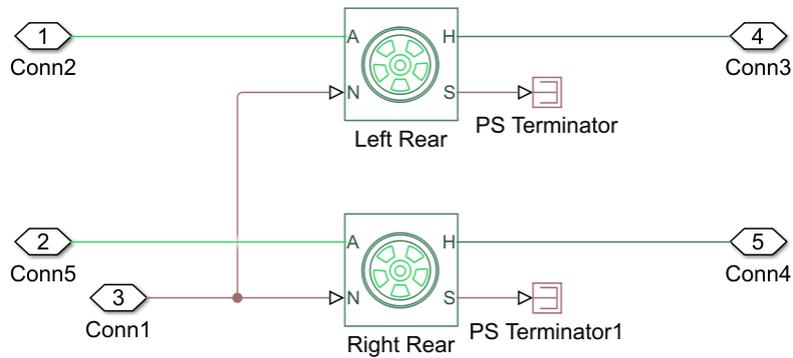
52

3.2.8   Rear axle

Figure 3.25 Simulink rear axle model

The rear axle (Figure 3.25) includes independent blocks of the left and rear wheels. The resulting torque from the differential is converted into the longitudinal force based on the geometric parameters of the tire, the type of surface and the grip coefficient with it. Created longitudinal force is connected to the vehicle body and moves it in the direction of the vector of the specified force.
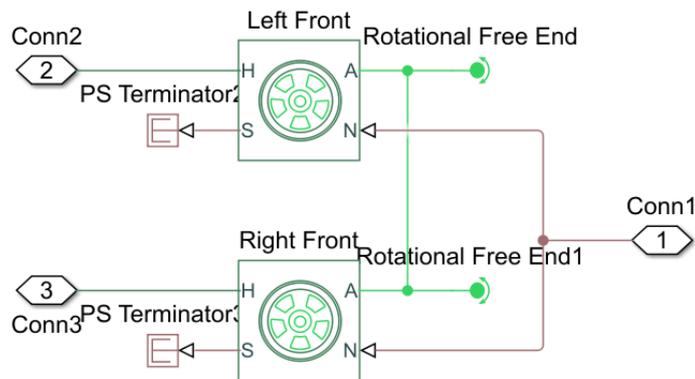
3.2.9   Front axle

Figure 3.26 Simulink front axle model

The front axle (Figure 3.26) is modeled in the same way as the rear axle. The difference if that the torque does not come directly from the engine, but through the rear axle systems.

3.3 Practical measurements and verification

In order to check the correctness of the model and verify it, two studies were conducted. The first one is a simulation of the linear movement of the Mitubishi i-MiEV HA3W. This car is chosen because it is the base for the ISEAUTO. All propulsion and chassis elements were taken from it, except vehicle body. In simulation general dimensions, front area, mass characteristics and air drag coefficient were set in accordance with the car manufacturer's specification. After that the maximum possible speed of movement and the acceleration time to 100 km/h were found (Figure 3.27). The obtained simulation data and the information provided by the manufacturer are shown in the Table 3.22.
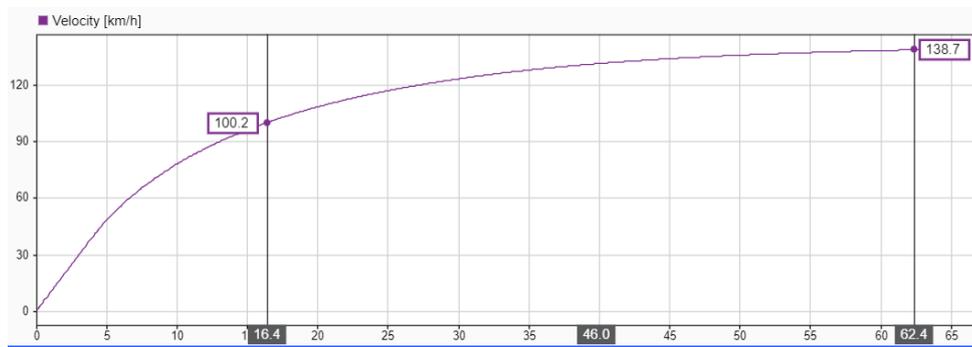

Figure 3.27 Mitubishi i-MiEV HA3W simulation

Table 3.22 Comparison table of theoretical and practical values

Parameter	Manufacturer data	Simulation	Error
Maximum speed, km/h	130	138	5,80%
Acceleration time to 100 km/h, s	15,9	16,4	3,14%

As can be seen from the obtained results, the error is relatively small. Of course, it should be taken into account that certain simplifications and assumptions were deliberately made in the dynamic calculations, that affects the accuracy of the data. Based on this, it can be confirmed that the model has successfully passed the first verification.

The second verification study consisted of receiving real measurements from ISEAUTO motion and compared with the theoretical expected results.

For this, three measurements were taken at the start of movement and acceleration up to 10 km/h and five measurements for complete stop. The speed of 10 km/h is chosen because ISEAUTO is still in the process of testing and its velocity is deliberately limited to 10 km/h.

ISEAUTO is controlled from a joystick that connects to the control unit. The throttle is regulated by the joystick slider and has a range of 0-1. At 0, no signals are sent to the motor, and at 1- current and voltage are supplied to the motor to obtain the maximum torque.

The feedback from movement characteristics consists from throttle input and the vehicle speed at each moment of time. The feedback step is approximately 20ms.

Having the dependence of the vehicle speed from the rate of pressing the throttle slider, the same conditions were set in the simulation using the signal builder (Figure 3.27). The change in torque in the simulation exactly copies the measured readings.
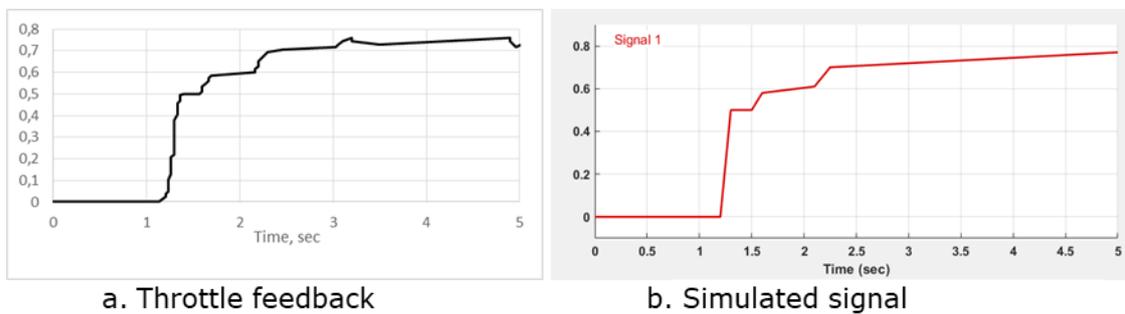All the measurements were carried out on a flat dry asphalt without a slope.

a. Throttle feedback   b. Simulated signal

Figure 3.28 Throttle feedback simulation

The first acceleration measurement

Results of the measurement are presented on the Figure 3.28.
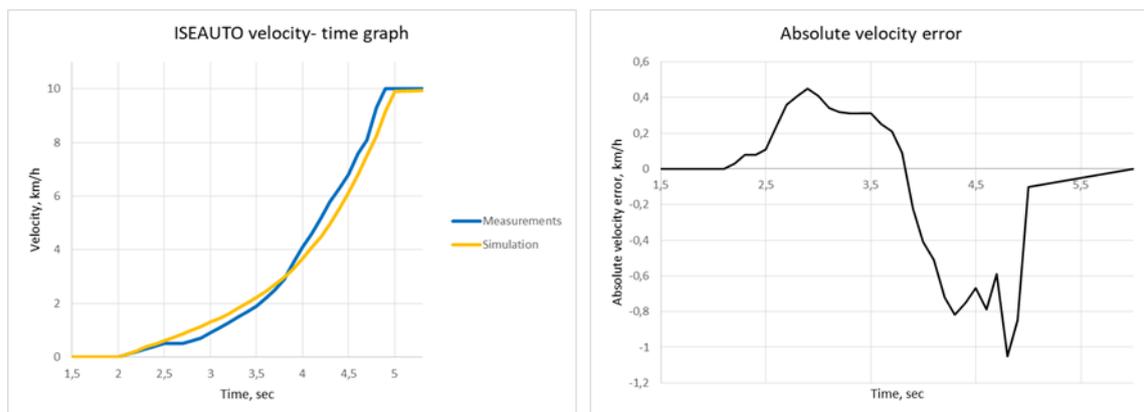

Figure 3.28 First measurements result

The difference in time of reaching 10 km/h between theoretical and practical results is only 0,1 sec. Despite this, the theoretical curve has a smoother pattern. The error has

the greatest value of approximately 1 km/h for a short period of time. Generally, the results of first measurement can be considered as completely satisfactory.

The second acceleration measurement

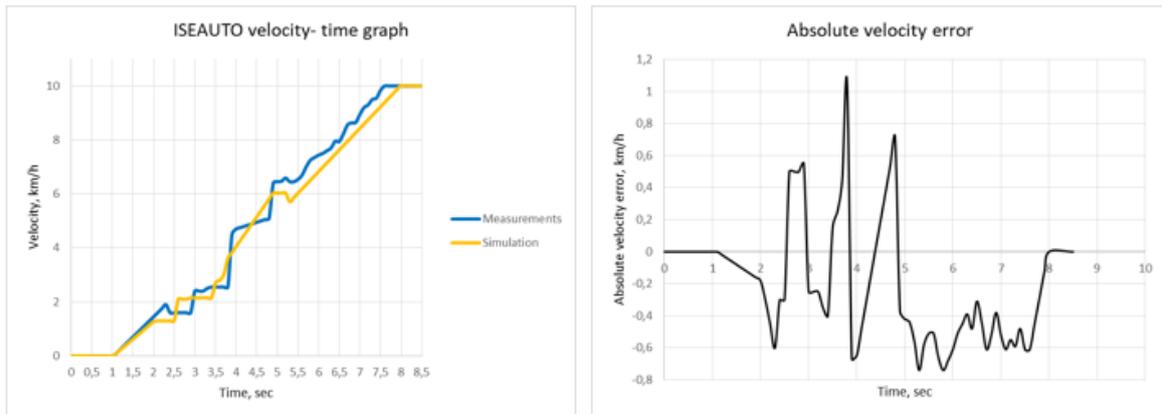Results of the measurement are presented on the Figure 3.29.

Figure 3.29 Second measurements result

The difference in time of reaching 10 km/h between theoretical and practical results is 0,4 sec. As in the previous measurement, the practical data have a more stepped pattern. The error has the greatest value of approximately 1,1 km/h for a short period of time. These results are satisfactory.

The third acceleration measurement

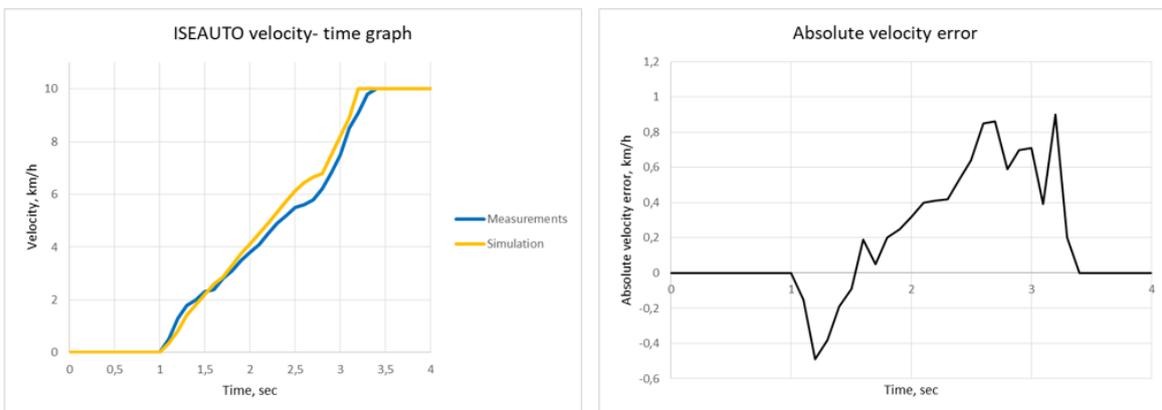Results of the measurement are presented on the Figure 3.30.

Figure 3.30 Third measurements result

The difference in time of reaching 10 km/h between theoretical and practical results is 0,2 sec. Unlike the previous two measurements, the simulation results outpaced the

practical measurements. The error has the greatest value of approximately 0,9 km/h for a short period of time. The results can be considered satisfactory.

Breaking measurement

The difficulty in conducting practical braking measurements is that it is impossible to trace exact signal strength. Moreover, the pressure applied to the brake pads can also vary greatly due to the emergency braking condition. In this case, five practical measurements were obtained practically and one theoretical in the condition of fully pressed break from the speed of 10 km/h. Data presented in Table 3.22.

Table 3.22 Time until full stop from 10 km/h

Practical stopping time, sec	Simulation stopping time, sec
1,2	
0,96	
0,84	0,8
0,82	
0,76	

As can be seen from the obtained results, the practical value is in the range of 0,76-1,20 sec, while the calculated stopping time is 0.8 sec. This deviation is caused by the inaccuracy of the input, which can be improved in the future for more precise results.

4 SUMMARY

In this work, dynamic model of the linear motion for the vehicle ISEAUTO was developed. This model takes into account the following characteristics:
- Mass: location of the centre of mass, axle load;
- dimensions: size, body profile area, distances to axles from the centre of mass;
- inertial: the inertia of all main moving units;
- air resistance;
- motor: torque - speed dependence, efficiency;
- transmission: inertia, efficiency;
- tires: type, size, static and kinetic friction, grip rate;
- road surface: type and condition;

Correctness of the developed model was verified in several ways:
- Acceleration simulation of Mitubishi i-MiEV HA3W. Results were compared with the manufacturer's stated specification. The model was fully verified;
- comparison of the acceleration curve from the throttling level on the real ISEAUTO and its dynamic model. The model was fully verified;
- comparison of stopping time from 10 km/h on the real ISEAUTO and its dynamic model. The results are considered enough accurate.

The developed model can be used for the following purposes:
- Analysis of linear motion ISEAUTO and prediction it`s behaviour at any time;
- trace the change in driving dynamics in case of replacing any components;
- optimization of autonomous driving to reduce losses and increase safety.

5 KOKKUVÕTE

Selles töös töötati välja ISEAUTO sõiduki lineaarse liikumise dünaamiline mudel. Selles mudelis võetakse arvesse järgmisi omadusi:

- Mass: massikeskme asukoht, teljekoormus;
- mõõtmed: suurus, kereprofiili pindala, kaugus telgedest massikeskmest;
- inerts: kõigi peamiste liikuvate üksuste inerts;
- õhutakistus;
- mootor: pöördemoment - sõltuvus kiirusest, efektiivsus;
- ülekanne: inerts, efektiivsus;
- rehvid: tüüp, suurus, staatiline ja kineetiline hõõrdumine, haardumine;
- teekate: tüüp ja seisukord;

Väljatöötatud mudeli korrektsust kontrolliti mitmel viisil:

- Mitubishi i-MiEV HA3W kiirendussimulatsioon. Tulemusi võrreldi tootja esitatud spetsifikatsiooniga. Mudel oli täielikult kontrollitud;
- tegeliku ISEAUTO ja selle dünaamilise mudeli kiirenduskõvera võrdlemine. Mudel oli täielikult kontrollitud;
- tegeliku ISEAUTO ja selle dünaamilise mudeli puhul peatumisaegade võrdlus alates 10 km / h. Tulemusi võib pidada üsna täpseteks.

Välja töötatud mudelit saab kasutada järgmistel eesmärkidel:

- lineaarse liikumise ISEAUTO analüüs ja selle käitumise ennustamine igal ajal;
- jälgida sõidudünaamika muutust komponentide vahetamise korral;
- autonoomse sõidu optimeerimine kadude vähendamiseks ja ohutuse suurendamiseks.

LIST OF REFERENCES

[1] A. Rathi, "Why the Cars of Our Self-Driving Future Will Be Electric," Bloomberg Green, July 7, 2020. [Online]. Available: https://www.bloomberg.com/news/articles/2020-07-07/self-driving-fully-electric-cars-will-be-the-ultimate-green-move

[2] J.Lanhee Lee, N.Frandino, "Self-driving vehicles get in on the delivery scene amid COVID-19", February 22. [Online]. Available: https://www.reuters.com/article/us-health-coronavirus-self-driving-deliv-idUSKBN22B2LZ

[3] B. Kamalakkannan, "Modelling and Simulation of Vehicle Kinematics and Dynamics," M.S. thesis, Halmstad University, 2017.

[4] Z. Wang, J. Wu, L. Zhang and Y. Wang, "Vehicle sideslip angle estimation for a four-wheel-independent-drive electric vehicle based on a hybrid estimator and a moving polynomial Kalman smoother," Journal of Multi-body Dynamics, vol. 234, p. 125–140, April 2018.

[5] M. Hamed, B. Tesfa, F. Gu and A.D.Ball, "Effects of Tyre Pressure on Vehicle Suspension Performance Effects of Tyre Pressure on Vehicle Suspension Performance," International Letters of Chemistry Physics and Astronomy, vol. 55, p. 104-113, July 2015.

[6] K. Parczewski, "Effect of tyre inflation pressure on the vehicle dynamics during braking manoeuvre," Eksploatacja i Niezawodnosc – Maintenance and Reliability, vol. 15, n. 2, p. 134–139, January 2013.

[7] Y. Nakajima, Advanced Tire Mechanics, Springer, pp-807-908, 2019.

[8] M. K. Ghezzi, "Control of a Four In-Wheel Motor Drive Electric Vehicle," M.S. thesis, Polytechnic University of Catalonia, 2017.

[9] H. B. Pacejka, Tyre and Vehicle Dynamics, Butterworth-Heinemann, 2002.

[10] M. A. Abdullah, J. F. Jamil, A. E. Mohan "Vehicle Dynamics Modeling & Simulation", Centre for Advanced Research on Energy, Faculty of Mechanical Engineering, Universiti Teknikal Malaysia Melaka, September 2016

[11] B. Zhang, J. Zhang, J. Yi, N. Zhang, Q. Jin "Modal and Dynamic Analysis of a Vehicle with Kinetic Dynamic Suspension System," Shock and Vibration, vol. 2016, February 2016.

[12] R. N. Jazar, Vehicle Dynamics, Springer, 2008.

[13] T. D. Gillespie, Fundamentals of Vehicle Dynamics. SAE International, 1992.

[14] S. Soylu, Electric Vehicles – Modelling and Simulations. IntechOpen, 2011.

[15] V.T.Minh, J.Pumwa, "Feasible Path Planning for Autonomous Vehicles," Mathematical Problems in Engineering, vol. 2014, March 2014.

[16] M. Guiggiani, The Science of Vehicle Dynamics. Handling, Braking, and Ride of Road and Race Cars, Springer, 2014.

[17] А. Шадин, Математическая модель разгона автомобиля с пробуксовкой ведущей оси, Publisher ФГБОУ ВПО "МГТУ им. Н.Э. Баумана". Эл № ФС 77 – 48211, 2008.

[18] F. Ahmad, S.A. Mazlan, Zamzuri H. Modelling and validation of the vehicle longitudinal model, International Journal of Automotive and Mechanical Engineering, 10(1):2042-2056, 2014.

[19] V.Thanh, V.T. Minh, "A Universal Dynamic and Kinematic Model of Vehicles", IEEE Vehicle Power and Propulsion Conference (VPPC), December 2015.

[20] Cheng Lin, Zhifeng Xu, "Wheel Torque Distribution of Four-Wheel-Drive Electric Vehicles Based on Multi-Objective Optimization", Energies 2015, vol. 8, pp. 3815-3831, April 2015.

[21] Bruce P. Minaker, Fundamentals of Vehicle Dynamics and Modelling: A Textbook for Engineers With Illustrations and Examples, Wiley, Dec 2019.

[22] A. Rassõlkin, T. Vaimann, A. Kallaste, R. Sell, "Propulsion Motor Drive Topology Selection for Further Development of ISEAUTO Self-Driving Car," IEEE 59th International Scientific Conference on Power and Electrical Engineering of Riga Technical University (RTUCON), 2018,

[23] I-MiEV Technical information manual, 2013. [Online]. Available:http://mmc-manuals.ru/manuals/i-miev/online/Service_Manual/2013/index_M2.html. [Accessed May, 2021]

[24] Rick Russo, "Differential and Planetary gear units," 17 July 2020. [Online]. Available: https://club.mobilindustrial.com/lube_talk/b/tip_of_the_week/posts/part-one-differential-and-planetary-gear-units [Accessed May, 2021].

[25] Kikas, "Road to TalTech ISEAUTO. 1/4: Dismantling the Mitsubishi i-Miev," 18 Sept 2018. [Online]. Available: https://iot.ttu.ee/iseauto-saamislugu-1/ [Accessed May, 2021].

[26] H. Heisler, "Brake system," Advanced Vehicle Technology (Second edition), 2002 [Online]. Available: https://www.sciencedirect.com/topics/engineering/brake-system [Accessed May, 2021].

[27] H. Pacejka, E. Bakker, L. Nyborg, "Tire modeling for use in vehicle dynamics studies", SAE Paper No. 870421, 1987.

APPENDICES

```matlab
%% Parameters
inclination_deg= 0; %%[deg]
wind_vel= 0; %%[m/s]

%% mass and center of mass
mass_shell=550; %%[kg]
mass_motor=90; %%[kg]
mass_batteries= 250; %%[kg]
mass_steering= 60; %%[kg]
mass_axleFwd=100; %%[kg]
mass_axleAft=120; %%[kg]
mass_passangers=400; %%[kg] 400

coord_shell = [1220,0,1540]; %%[x;y;z]
coord_motor = [2550,0,350]; %%[x;y;z]
coord_batteries = [1420,0,150]; %%[x;y;z]
coord_steering = [0,0,350]; %%[x;y;z]
coord_axleFwd = [0,0,0]; %%[x;y;z]
coord_axleAft = [2550,0,0]; %%[x;y;z]
coord_passangers = [1550,0,870]; %%[x;y;z]
%% Vehicle parameters
drag_coeff= 0.7; %%
front_area = 3.6; %%m2
%% Tire parameters (dry surface)
frontTire_mass =7;
frontTire_fitD = 381; %%tire fit diameter [mm]
frontTire_H = 94;  %%tire profile height [mm]
frontTire_W = 145; %%tire width [mm]

rearTire_mass =10;
rearTire_fitD = 381; %%tire fit diameter [mm]
rearTire_H = 96;  %%tire profile height [mm]
rearTire_W = 175; %%tire width [mm]

load_coeff= 0.85 %% 0.85-0.9 for diagonal tires, 0.8-0.85
for radial tires

surface= 'dry';%% dry/wet/snow/ice

roll_resist = 0.0062;

%% Breaking
```

```
maxBreakingPressure = 10.8*10^9 %% Pa
BreakingPressure = 0 %% Pa
    %%Rear Breaking
cylD_rearBR = 19.1 %%mm Wheel cylinder diameter

dram_R_rearBR= 150; %%mm
act_R_rearBR = 100; %%mm
pin_loc_rearBR = 125; %%mm
pin_angle_rearBR = 15; %%deg
shoe_angle_rearBR= 5; %%deg
shoe_span_rearBR= 120; %%deg
viscFriction_coef_rearBR=0.01; %%N*m/(rad/s)
contFriction_coef_rearBR=0.3;
    %%Front Breaking
pad_R_frontBR = 150; %%[mm] mean radius of brake pad force
application on brake rotor
cylinder_bore_frontBR = 10 %%[mm]  brake actuator bore
diameter.
num_pads_frontBR = 2 %%number of brake pads in disc brake
assembly

static_friction_coeff_frontBR =  0.3;  %%disc pad-rotor
coefficient of static friction.
coloumb_friction_coeff_frontBR = 0.3;  %%disc pad-rotor
coefficient of kinetic friction.
viscFriction_coef_rearBR = 0.01; %%N*m/(rad/s)

%% Transmission
GearRatio = 6.066;
input_shaft_mass= 3.5; %%kg
input_shaft_inertia = 0.00504;%%kg*m^2

output_shaft_mass= 3.2; %%kg
output_shaft_inertia = 0.03412; %%kg*m^2

gear1_m = 8; %%kg
gear1_d = 170; %%mm

gear2_m = 2.5; %%kg
gear2_d = 50; %%mm

gear3_m = 3.5; %%kg
gear3_d = 90; %%mm

gear4_m = 2.5; %%kg
gear4_d = 50; %%mm
```

```matlab
trans_eff= 0.85;%% transmission efficiency

diff_eff = 0.92;%% differencial efficiency
%% inertia moments

engine_Inertia = 0.012 %%kg*m^2 19.003
differential_Inertia= 0.0361; %%kg*m^2
RearAxle_Inertia= 0.138; %%kg*m^2
FrontAxle_Inertia= 0.138; %%kg*m^2

%% Front suspension
d_sprinf_fwd= 10*10^(-3); %%diameter of spring wire (m)
D_sprinf_fwd= 86*10^(-3); %%Diameter of spring (mm)
Shear_modulus= 11500000;  %%shear modulus of elasticity
of the spring material (11,500,000 for a steel spring)
Num_coils_fwd= 5;   %%number of active coils
stiffenes_fwd= 770.9; %%spring stiffness [N/m]

%% Rear suspension
d_sprinf_rear= 11*10^(-3) %%diameter of spring wire (m)
D_sprinf_rear= 97*10^(-3) %%Diameter of spring (mm)
Shear_modulus= 11500000  %%shear modulus of elasticity of
the spring material (11,500,000 for a steel spring)
Num_coils_rear= 5   %%number of active coils
stiffenes_rear= 1264.8 %%spring stiffness [N/m]

%% Longitudinal-lateral dynamics

Angle_left_wheel= 15;
Angle_right_wheel = 17;
Angle_steering        =        (Angle_left_wheel       +
Angle_right_wheel)/2;

%% Calculations
inclination_rad= inclination_deg*pi/180; %%[rad]

mass_total= mass_shell + mass_motor + mass_batteries +
mass_axleFwd + mass_axleAft + mass_passangers;
coord_cm=
(coord_shell*mass_shell+coord_motor*mass_motor+coord_bat
teries*mass_batteries+coord_steering*mass_steering+coord
_axleFwd*mass_axleFwd+coord_axleAft*mass_axleAft      +
coord_passangers*mass_passangers)/mass_total;
vehicle_mass = mass_total - mass_passangers;
massLoad_axleFwd=
mass_total/(coord_cm(1)/(coord_axleAft(1)-
coord_cm(1))+1);
massLoad_axleAft= mass_total- massLoad_axleFwd;
```

```matlab
CG_height = coord_cm(3); %%mm
front_axle= coord_cm(1); %%mm
rear_axle= coord_axleAft(1)-coord_cm(1); %%mm

frontTire_R = frontTire_fitD/2+ frontTire_H;   %%outer
tire radius [mm]
rearTire_R = rearTire_fitD/2+ rearTire_H;  %%outer tire
radius [mm]

front_tire_R_static=
0.5*frontTire_fitD+frontTire_H*load_coeff    %%    static
radius, mm
rear_tire_R_static=
0.5*rearTire_fitD+rearTire_H*load_coeff %% static radius,
mm

switch surface
    case 'dry'
        tire_b= 10; tire_c= 1.9; tire_d= 1; tire_e= 0.97;
    case 'wet'
        tire_b= 12; tire_c= 2.3; tire_d= 0.82; tire_e= 1;
    case 'snow'
        tire_b= 5; tire_c= 2; tire_d= 0.3; tire_e= 1;
    case 'ice'
        tire_b= 4; tire_c= 2; tire_d= 0.1; tire_e= 1;
end

frontTire_inertia=
1/2*rearTire_mass*((frontTire_R/1000)^2+(frontTire_fitD)
/1000^2) ; %% inertia of front tire, N*m
rearTire_inertia=
1/2*frontTire_mass*((rearTire_R/1000)^2+(rearTire_fitD)/
1000^2) ; %% inertia of rear tire, N*m

veh_length= 3560; l= veh_length/1000;
veh_width = 2358; w= veh_width/1000;
veh_height = 1588; h= veh_height/1000;
m= mass_total;

I_x= (0.79*m)*(w^2+h^2)/12-12.085; %%roll moment
I_y= (0.79*m)*(l^2+h^2)/12-12.085; %% pitch moment
I_z= (0.79*m)*(l^2+w^2)/12-12.085; %% yaw moment

gear1_Inertia=gear1_m*(gear1_d*10^(-3))^2/4; %%kg*m^2
gear2_Inertia=gear2_m*(gear2_d*10^(-3))^2/4; %%kg*m^2
gear3_Inertia=gear3_m*(gear3_d*10^(-3))^2/4; %%kg*m^2
gear4_Inertia=gear4_m*(gear4_d*10^(-3))^2/4; %%kg*m^2
```

```matlab
maxForce_rearBR                            =
maxBreakingPressure*pi*(cylD_rearBR*10^(-3))^2;        %%N
maximum force

gearbox_Inertia=
gear1_Inertia+gear2_Inertia+gear3_Inertia+gear4_Inertia;
%%kg*m^2

l_fwd= coord_cm(1)-coord_axleFwd(1);
l_aft= coord_cm(1)-coord_axleAft(1);

inertia_shell=1732.57; %%[kg*m2]
inertia_motor=mass_motor*abs((coord_cm(1)-
coord_motor(1)))^2*10^-6; %%[kg*m2]
inertia_batteries=     mass_batteries*abs((coord_cm(1)-
coord_motor(1)))^2*10^-6; %%[kg*m2]
inertia_steering=       mass_steering*abs((coord_cm(1)-
coord_motor(1)))^2*10^-6; %%[kg*m2]
inertia_axleFwd=mass_axleFwd*abs((coord_cm(1)-
coord_axleFwd(1)))^2*10^-6; %%[kg*m2]
inertia_axleAft=mass_axleAft*abs((coord_cm(1)-
coord_axleAft(1)))^2*10^-6; %%[kg*m2]
inertia_passangers=mass_passangers*abs((coord_cm(1)-
coord_passangers(1)))^2*10^-6; %%[kg*m2]

pitch_inertia=
inertia_shell+inertia_motor+inertia_batteries+inertia_st
eering+inertia_axleFwd+inertia_axleFwd+inertia_axleAft+i
nertia_passangers
```

Name ▲	Value	Name ▲	Value
act_R_rearBR	100	frontTire_H	94
Angle_left_wh...	15	frontTire_inertia	0.4066
Angle_right_w...	17	frontTire_mass	7
Angle_steering	16	frontTire_R	284.5000
ans	6	frontTire_W	145
BreakingPress...	0	gear1_d	170
CG_height	850.9934	gear1_Inertia	0.0578
coloumb_frict...	0.3000	gear1_m	8
contFriction_c...	0.3000	gear2_d	50
coord_axleAft	[2550,0,0]	gear2_Inertia	0.0016
coord_axleFwd	[0,0,0]	gear2_m	2.5000
coord_batteri...	[1420,0,150]	gear3_d	90
coord_cm	[1.4447e+03,0,85...	gear3_Inertia	0.0071
coord_motor	[2550,0,350]	gear3_m	3.5000
coord_passan...	[1550,0,870]	gear4_d	50
coord_shell	[1220,0,1540]	gear4_Inertia	0.0016
coord_steering	[0,0,350]	gear4_m	2.5000
cylD_rearBR	19.1000	gearbox_Inertia	0.0680
cylinder_bore...	10	GearRatio	6.0660
d_sprinf_fwd	0.0100	h	1.5880
D_sprinf_fwd	0.0860	I_x	791.3240
d_sprinf_rear	0.0110	I_y	1.4985e+03
D_sprinf_rear	0.0970	I_z	1.8005e+03
diff_eff	0.9200	inclination_deg	0
differential_In...	0.0361	inclination_rad	0
drag_coeff	0.7000	inertia_axleAft	146.6020
dram_R_rearBR	150	inertia_axleFwd	208.7164
engine_Inertia	0.0120	inertia_batteries	305.4209
front_area	3.6000	inertia_motor	109.9515
front_axle	1.4447e+03	inertia_passang...	4.4351
front_tire_R_st...	270.4000	inertia_shell	1.7326e+03
FrontAxle_Ine...	0.1380	inertia_steering	73.3010
frontTire_fitD	381	input_shaft_iner...	0.0050
frontTire_H	94	input_shaft_mass	3.5000

Name ▲	Value	Name ▲	Value
input_shaft_mass	3.5000	pin_loc_rearBR	125
l	3.5600	pitch_inertia	2.7897e+03
l_aft	-1.1053e+03	rear_axle	1.1053e+03
l_fwd	1.4447e+03	rear_tire_R_static	272.1000
load_coeff	0.8500	RearAxle_Inertia	0.1380
logsout_cvtMod…	1x1 Dataset	rearTire_fitD	381
m	1510	rearTire_H	96
m1	3.5000	rearTire_inertia	0.2886
m2	3.2000	rearTire_mass	10
mass_axleAft	120	rearTire_R	286.5000
mass_axleFwd	100	rearTire_W	175
mass_batteries	250	roll_resist	0.0062
mass_motor	90	rpmVector	[1;2000;2500;300…
mass_passangers	400	Shear_modulus	11500000
mass_shell	550	shoe_angle_rear…	5
mass_steering	60	shoe_span_rear…	120
mass_total	1510	simlog_cvtMod…	1x1 Node
massLoad_axle…	855.4902	speedVector	70x1 double
massLoad_axleF…	654.5098	static_friction_c…	0.3000
maxBreakingPre…	1.0800e+10	stiffenes_fwd	770.9000
maxForce_rearBR	1.2378e+07	stiffenes_rear	1.2648e+03
mr1	0.8000	surface	'dry'
mr2	0.7000	tire_b	10
Num_coils_fwd	5	tire_c	1.9000
Num_coils_rear	5	tire_d	1
num_pads_front…	2	tire_e	0.9700
output_shaft_in…	0.0341	torqueVector	[50;50;50;50;30;1…
output_shaft_m…	3.2000	trans_eff	0.8500
pad_R_frontBR	150	veh_height	1588
pin_angle_rearBR	15	veh_length	3560
pin_loc_rearBR	125	veh_width	2358
pitch_inertia	2.7897e+03	vehicle_mass	1110
rear_axle	1.1053e+03	viscFriction_coe…	0.0100
rear_tire_R_static	272.1000	w	2.3580
		wind_vel	0